	X-ray tests at PANTER on Nickel-Cobalt EM#3 (phase A) SIMBOL-X optic prototype					
Code:01/2009	INAF/OAB Technical Report	Issue:	2	Class	CONFIDENTIAL	Page: 1

X-ray tests at PANTER on Nickel-Cobalt EM#3 (phase A) SIMBOL-X optic prototype

*Issued by **D. Spiga** (INAF/OAB)*

*Full-illumination X-ray measurements performed by the PANTER team: **M. Freyberg, W. Burkert, G. Hartner, B. Budau** (MPE Garching, Germany)*


*Multilayer coatings deposited under supervision of **V. Mattarello, D. Garoli, E. Boscolo Marchi** (Media-Lario techn.)*

*Mirrors integration and UV measurements by **S. Basso, R. Valtolina** (INAF/OAB)*

*Support hardware design, manufacturing and mounting by **E. Mattaini** (INAF/IASF Milano), **S. Basso, R. Canestrari, D. Garegnani, R. Valtolina** (INAF/OAB)*

*Reviewed by **G. Tagliaferri, G. Pareschi, A. Moretti** (INAF/OAB)*

Istituto Nazionale di Astrofisica (INAF)
 Via del Parco Mellini, 00100 Roma, Italy
Osservatorio Astronomico di Brera (OAB)
 Via Brera 28, 20121 Milano, Italy
 Via E. Bianchi 46, 23807 Merate, Italy

	X-ray tests at PANTER on Nickel-Cobalt EM#3 (phase A) SIMBOL-X optic prototype						
Code:01/2009	INAF/OAB Technical Report	Issue:	2	Class	CONFIDENTIAL	Page:	2

Contents


1. Introduction.....	4
2. Preliminary analyses.....	6
2.1. On-axis geometric properties.....	6
2.2. Multilayer structure	10
2.3. Off-axis EA predictions	10
3. System alignment and best foci.....	12
4. Mirror shell 286.....	15
4.1. The PSPC and TRoPIC views	15
4.2. Effective areas.....	17
4.2.1. On-axis EA	18
4.2.2. Off-axis EA	19
4.3. HEW and W90.....	20
5. Mirror shell 291 and 295.....	23
5.1. The PSPC and TRoPIC views	23
5.2. Effective areas.....	25
5.2.1. On-axis EA	25
5.2.2. Off-axis EA	26
5.3. HEW and W90.....	27
6. Complete EM#3 optic (286+291+295).....	29
6.1. The PSPC and TRoPIC views	29
6.2. Effective Areas	31
6.2.1. On-axis EA	31
6.2.2. Off-axis EA	33
6.3. HEW and W90.....	34
7. Final remarks	37

Applicable Documents

- [AD1] *NHXM Optical Payload Preliminary Development Plan & Model Philosophy*, MLT Technical note SX-PL-ML-003 (2007)
- [AD2] D. Spiga, F. Mazzoleni et al., *Mirror shell 295/2 for SIMBOL-X optic Phase A prototype: results of performed tests at MPE-PANTER*. INAF/OAB Technical report 04/2008
- [AD3] D. Spiga, E. Dell'Orto et al., *X-ray tests at PANTER on the optic 291+295 prototype (EM#1) for the phase A of SIMBOL-X*, INAF/OAB internal report 07/2008
- [AD4] D. Spiga et al., *X-ray tests at PANTER on the EM#2 SIMBOL-X optic (phase A)*, INAF/OAB internal report 09/2008

Reference Documents


- [RD1] M. Freyberg et al., *The MPE X-ray test facility PANTER: calibration of hard X- ray (15-50 keV) optics* - **Experimental Astronomy**, vol. 20, 1-3 (2006)
- [RD2] G. Pareschi, P. Ferrando, *The SIMBOL-X hard X-ray mission*. **Exp. Astron.** 20, 139-149 (2006)
- [RD3] D. Spiga et al., *Characterization of Pt/C and W/Si multilayer-coated mirror shells at the PANTER facility*, OAB Internal Report 07/05 (2005)
- [RD4] S. Basso, *Geometrical tolerances for mandrel design*, OAB Internal Report 06/2008 (2008)

	X-ray tests at PANTER on Nickel-Cobalt EM#3 (phase A) SIMBOL-X optic prototype						
Code:01/2009	INAF/OAB Technical Report	Issue:	2	Class	CONFIDENTIAL	Page:	3

- [RD5] L. Strüder et al., *The European Photon Imaging Camera on XMM-Newton: The pn-CCD Camera*, **Astronomy and Astrophysics** 365, L18-L26 (2001)
- [RD6] P. Predehl et al., *eROSITA*, **SPIE Proc.** 62660P (2006)
- [RD7] L. P. Van Speybroeck and R. C. Chase, *Design Parameters of Paraboloid-Hyperboloid Telescopes for X-ray Astronomy*, **Appl. Opt.**, 11(2) 440-445 (1972)

Acronyms

AFM	Atomic Force Microscope
CfA	Harvard- Smithsonian Center for Astrophysics
CCD	Charge-Coupling Device
EA	Effective Area
EM	Engineering Model
FOV	Field Of View
f.c.	for comparison
HEW	Half-Energy Width
INAF	Istituto Nazionale di AstroFisica / <i>Italian Institute for Astrophysics</i>
I. P.	Intersection Plane
MLT	Media-Lario Technologies
MPE	Max-Planck Institut für Extraterrestrische Physik / <i>Max Planck Institute for Extraterrestrial Physics</i>
MS	Mirror Shell
NiCo	Nickel-Cobalt
OAB	Osservatorio Astronomico di Brera / <i>Brera Astronomical Observatory</i>
OOF	Out-Of-Focus
PSPC	Position-Sensitive Proportional Counter
ROI	Region of Interest
UV	UltraViolet
wrt.	with respect to
XRR	X-ray Reflectivity
XRS	X-ray Scattering
VOB	Vertical Optical Bench

	X-ray tests at PANTER on Nickel-Cobalt EM#3 (phase A) SIMBOL-X optic prototype					
Code:01/2009	INAF/OAB Technical Report	Issue:	2	Class	CONFIDENTIAL	Page: 4

1. Introduction


The present document reports the results of the measurement campaign at the MPE-PANTER [RD1] facility (Neuried bei München, Germany) on an optic prototype for the Phase A of the SIMBOL-X hard X-ray telescope development project [AD1, RD2]. The optic prototype (named EM#3) consists of 3 nested and confocal mirror shells, replicated at *Media-Lario techn.* from Kanigen-coated mandrel polished at INAF/OAB. The shells have been replicated from the same mandrels used for the previous tests of this study [AD2, AD3, AD4], but they are made of a **Nickel-Cobalt** (NiCo) alloy, rather than simple Nickel adopted hitherto. The advantage of the NiCo alloy resides in its nearly-amorphous bulk structure (suggested also by their the shiny, silvery colour): this results in a lower microstress of shell and coating, wrt. the polycrystalline texture of Nickel. This is expected to extend the elastic regime of the material, making it less sensitive to permanent deformations that might arise at the electroforming and release stage of the mirror replication from a mandrel. Moreover, a less strained texture would likely result in a smoother optical surface: this means that the electroforming and release process is expected to develop a smaller roughness.

Like the previous prototypes, mirrors have been coated with a graded W/Si multilayer that enhances their reflectivity in the hard X-ray band, up to 50 keV. These multilayer coatings, deposited by RF magnetron sputtering at MLT using a developed facility [AD1] for this project, have all the same nominal structure adopted in the EM#2 tests campaign [AD4]. The three coated mirror shells have then been integrated at the VOB at INAF/OAB in their integration case, while their HEW was monitored and minimized in UV light (373 nm).

The diameters of mirror shells are approx. 286, 291 and 295 mm at their principal plane (refer to next section for more precise information). In the following we shall refer to them as *MS286/1* (1st replica from the same mandrel), *MS291/8* (8th replica) and *MS295/9* (9th replica), or simply MS286, MS291, MS295. The focal length are approx. 10 m, actually half focal length of SIMBOL-X optics. The nominal incidence angles, indeed, (0.205, 0.208, 0.211 deg) and the mirror wall thickness (250 μ m) are in the operational range of SIMBOL-X. The spider has 20 spokes, a number near that of SIMBOL-X (24). The mirrors are 600 mm long, the same length foreseen for SIMBOL-X. A picture of the EM#3 assembly, taken at the integration stage, is reported in Fig. 1.




Fig. 1:(left) a view of the EM3 during the integration. Notice the mutual closeness of the 3 mirror shells. (right) the final stage of the integration of the mirror shells. The temporary clamps, utilized to endow the shells with the necessary stiffness while handled, are being removed.

	X-ray tests at PANTER on Nickel-Cobalt EM#3 (phase A) SIMBOL-X optic prototype						
Code:01/2009	INAF/OAB Technical Report	Issue:	2	Class	CONFIDENTIAL	Page:	5

Several details, including the description of the optic mounting system and data reduction, can be retrieved from [AD2, AD3, AD4]. Note that, however, the 3 shells will not be measured all separately. Two shutters are implemented in the jig, one selecting/stopping the focused beam from the MS291 and MS295, whilst the other one selects the MS286 alone. In other words, the MS295 and the MS291 will be measured together at their best align and focus. In this series of tests we also executed off-axis measurements to check the imaging quality over the FOV of SIMBOL-X (6 arcmin radius).

In the following sections we report the measurements results of a) *focal lengths*, 2) *Effective Areas*, 3) *angular resolution* performed on the optic prototype at PANTER at 1 to 45 keV, using the the *PSPC* in monochromatic setup at low energies (< 10 keV) and with *TroPIC* at high energies (> 10 keV) in polychromatic setup. Several details regarding the measurement setup and the detectors can be retrieved from [AD3, RD5, RD6].

	X-ray tests at PANTER on Nickel-Cobalt EM#3 (phase A) SIMBOL-X optic prototype						
Code:01/2009	INAF/OAB Technical Report	Issue:	2	Class	CONFIDENTIAL	Page:	6

2. Preliminary analyses

2.1. On-axis geometric properties

We report hereafter (Tab. 1 to Tab. 3) some geometrical features of the mirror shells under test. The focal lengths and the HEWs were measured in UV light (373 nm) at the Brera VOB, using the new UV source provided by MLT.


1. *The 3 MSs have not the same focal length.* With respect to the focus of all the EM#3, that of the MS291 is the shortest (-30 mm), followed by the MS295 (-10 mm) and the MS286 (+10 mm). The situation is improved wrt. the EM#2 [AD4], whose shells had 2 focal lengths differing by 5 cm. The focal length is also closer to the nominal 10 m than for the EM#2, which results in slightly larger incidence angles.
2. *The 3 MSs are confocal.* The 3 foci at VOB coincide within 60 μm , much less than the pixel size of TROPIC at PANTER.
3. *The HEW of the 3 MSs is close to 20 arcsec.* At the respective best focus, after subtraction of the diffraction term, the MS295 has a 19.3 arcsec HEW, the MS286 has a 20.1 arcsec HEW, the MS291 has a 23.7 arcsec HEW. All the mirror assembly, at its best focus, has a 22.1 arcsec HEW. The same values were obtained with the VOB, within the experimental error, after the measurements at PANTER.
4. The focal length of the EM#3 that will be measured at PANTER is approximately 10.9 m due to the finite distance of the source [AD3].
5. For all shells, *the first half of the parabolic section will not be observed in double reflection* due to the finite distance of the source [AD3].
6. For all shells, *the incidence angles on the parabola and on the hyperbola are different*, also with the source on-axis, because of the non-negligible X-ray beam divergence [AD3].
7. The spider itself obstructs the 10% of the geometric (and effective) area.
8. Small Aluminium bars (5.35 mm large, 1.95 mm thick) have been glued to the front surfaces of the spider spokes (only a bit narrower than the bars) to shade their lateral surface against grazing incidence reflection [AD3]. This increases the spider obstruction, V , by an amount slightly variable with the energy of the photons (2%, due to the variable Aluminium transparency $T_{Al}(E)$):

$$V_{286}(E) = 0.1 + 0.019 \times (1 - T_{Al}(E)) \quad (2.1)$$

$$V_{291}(E) = 0.1 + 0.017 \times (1 - T_{Al}(E)) \quad (2.2)$$


$$V_{295}(E) = 0.1 + 0.015 \times (1 - T_{Al}(E)), \quad (2.3)$$

the transparency of the Aluminium bars, as a function of E , is plotted in [AD3].

	X-ray tests at PANTER on Nickel-Cobalt EM#3 (phase A) SIMBOL-X optic prototype						
Code:01/2009	INAF/OAB Technical Report	Issue:	2	Class	CONFIDENTIAL	Page: 7	


Tab. 1: Geometric properties of the shell 286/1

<i>Parameter</i>	<i>Symb.</i>	<i>Value</i>
Maximum mirror diameter (parabola)	$2R_{max}$	288.65 mm
Median mirror diameter	$2R_{med}$	286.50 mm
Minimum mirror diameter (hyperbola)	$2R_{min}$	280.07 mm
Mirror length (parabola + hyperbola)	$2L$	600 mm
Nominal, on-axis, <i>average</i> incidence angle	α	0.204 deg
Measured focal length with the VOB	f	$f_{EM\#3} + 1$ cm
Focal distance for a source at infinity (computed from PANTER meas.)	f	10.07 m
Mirror walls thickness	τ	250 μ m
No. of spider spokes	s	20
Expected figure error HEW (measured with the VOB at INAF/OAB)	H_0	20.1 arcsec
Distance of the X-ray source at PANTER	D	120.90 m
X-ray beam divergence (at the mirror front-end) at PANTER	δ	0.068 deg
Average incidence angle on the parabola at PANTER	α_P	0.272 deg
Average inc. angle on the hyperbola (for <i>double reflection</i>) at PANTER	α_H	0.136 deg
<i>Lost</i> area fraction of parabola for double reflection at PANTER	Q	49.7 %
Radius of the parabola single-reflection corona at PANTER	r_p	52.3 mm
Mirror obstruction by spider at 1 keV	V	11.89 %
Obstructed geometric cross-section for double reflection at PANTER	A_G^{hp}	5.71 cm²

	X-ray tests at PANTER on Nickel-Cobalt EM#3 (phase A) SIMBOL-X optic prototype						
Code:01/2009	INAF/OAB Technical Report	Issue:	2	Class	CONFIDENTIAL	Page:	8


Tab. 2: Geometric properties of the shell 291/8

<i>Parameter</i>	<i>Symb.</i>	<i>Value</i>
Maximum mirror diameter (parabola)	$2R_{max}$	293.20 mm
Median mirror diameter	$2R_{med}$	291.04 mm
Minimum mirror diameter (hyperbola)	$2R_{min}$	284.47 mm
Mirror length (parabola + hyperbola)	$2L$	600 mm
Nominal, on-axis, <i>average</i> incidence angle	α	0.208 deg
Measured focal length with the VOB	f	$f_{EM\#3}$ - 3 cm
Focal distance for a source at infinity (computed from PANTER meas.)	f	10.03 m
Mirror walls thickness	τ	250 μ m
No. of spider spokes	s	20
Expected figure error HEW (measured with the VOB at INAF/OAB)	H_0	23.7 arcsec
Distance of the X-ray source at PANTER	D	120.90 m
X-ray beam divergence (at the mirror front-end) at PANTER	δ	0.069 deg
Average incidence angle on the parabola at PANTER	α_p	0.277 deg
Average inc. angle on the hyperbola (for <i>double reflection</i>) at PANTER	α_H	0.139 deg
<i>Lost</i> area fraction of parabola for double reflection at PANTER	Q	49.3%
Radius of the parabola single-reflection corona at PANTER	r_p	53.1 mm
Mirror obstruction by spider (at 1 keV)	V	11.70 %
Obstructed geometric cross-section for double reflection at PANTER	A_G^{hp}	5.92 cm²

	X-ray tests at PANTER on Nickel-Cobalt EM#3 (phase A) SIMBOL-X optic prototype						
Code:01/2009	INAF/OAB Technical Report	Issue:	2	Class	CONFIDENTIAL	Page:	9

Tab. 3: Geometric properties of the shell 295/9

<i>Parameter</i>	<i>Symb.</i>	<i>Value</i>
Maximum mirror diameter (parabola)	$2R_{max}$	297.3 mm
Median mirror diameter	$2R_{med}$	295.1 mm
Minimum mirror diameter (hyperbola)	$2R_{min}$	288.4 mm
Mirror length (parabola + hyperbola)	$2L$	600 mm
Nominal, on-axis, <i>average</i> incidence angle	α	0.210 deg
Measured focal length with the VOB	f	$f_{EM\#3}$ - 1 cm
Focal length for a source at infinity (computed from PANTER meas.)	f	10.05 m
Mirror walls thickness	τ	250 μ m
No. of spider spokes	s	20
Expected figure error HEW (measured with the VOB at INAF/OAB)	H_0	19.3 arcsec
Distance of the X-ray source at PANTER	D	120.90 m
X-ray beam divergence (at the mirror front-end) at PANTER	δ	0.070°
Average incidence angle on the parabola at PANTER	α_p	0.280 deg
Average inc. angle on the hyperbola (for <i>double reflection</i>) at PANTER	α_H	0.140 deg
<i>Lost</i> area fraction of parabola for double reflection at PANTER	Q	49.7 %
Radius of the parabola single-reflection corona at PANTER	r_p	53.9 mm
Mirror obstruction by spider at 1 keV	V	11.54 %
Obstructed geometric cross-section for double reflection at PANTER	A_G^{hp}	6.09 cm²

	X-ray tests at PANTER on Nickel-Cobalt EM#3 (phase A) SIMBOL-X optic prototype						
Code:01/2009	INAF/OAB Technical Report	Issue:	2	Class	CONFIDENTIAL	Page:	10

2.2. Multilayer structure

The nominal structure of the multilayer is the same reported in [AD4]. As the deposition facility has targets as long as the mirror shell itself, there is no room to put a small substrate in front of the targets during the coating run of MS under test: the stack parameters (Tab. 4), that will be used to derive a theoretical model of the mirror shells EA, are the same derived from the analysis of a deposition run immediately previous to that of the MS295 of the EM#2.

Tab. 4: probable multilayer structure, as derived from the witness sample of the MS#295 of the EM#2

	Supermirror parameters for Si	Supermirror parameters for W
1 st power law (20 bilayers):	$A = 63.43 \text{ \AA}, b = -0.90, c = 0.31$	$a = 45.56 \text{ \AA}, b = -0.64, c = 0.294$
2 nd power law (75 bilayers)	$a = 60.3 \text{ \AA}, b = 27.6, c = 0.24$	$a = 19.72 \text{ \AA}, b = 1.15, c = 0.37$


A verification of the stability of these parameters over the time elapsed from EM#2 to EM#3 has also been done by measuring the reflectivity of a witness sample just outside the mirror shell length. Some previous runs allowed us establishing a nearly-constant thickness ratio between the sample placed outside the shell and samples aligned along the shell length. The tests allowed us to reasonably conclude that the Tab. 4 reports a good approximation to the actual multilayer structure.

The XRR measurement on the witness sample returns a roughness close to that of the Si wafer substrate (3 Å). The roughness of the multilayer on the MSs will then probably inherit the roughness of the substrate, without a relevant intrinsic contribution. Finally, notice that the W density inferred from the fit is lower (17.5 – 18 g/cm³) than the natural one (19.3 g/cm³). The inferred value for the density will be adopted in the following estimations.

2.3. Off-axis EA predictions

In this section we provide estimates of the mirror shell EAs that will be measured at PANTER. This will also include a quantification of the effects on the EA due to the off-axis setup:

- 1) *Mirror reflectivity variation with off-axis*: in addition to all the usual effects affecting the EA of the mirrors (finite distance of the source, obstructions, surface roughness), already accounted for in previous reports [AD2, AD3, AD4], we have to consider, this time, that the two MS291 and MS295 will be measured together, and in general they will not be *perfectly* mutually aligned at the integration stage. The EA simulation has to account for this effect, that changes the reflectivity of the mirrors, depending on their impact point on the shells, even on-axis. A probable mutual misalignment between the shells should not, indeed, exceed 70 arcsec, like for the EM#2 [AD4]. The effect of this misalignment is expectedly a smoothing of short-period reflectance features in the EA. For an off-axis setup, the situation is different because the reflectivity and the vignetting of the mirrors varies from point to point of the mirror.
- 2) *Spider obstruction*: the off-axis causes the two spiders not to be any longer aligned and their obstruction might be larger. However, this effect has a small impact. If there were no Aluminium bars on the spokes (Sect. 2.1), for a 0.1 deg maximum misalignment

	X-ray tests at PANTER on Nickel-Cobalt EM#3 (phase A) SIMBOL-X optic prototype						
Code:01/2009	INAF/OAB Technical Report	Issue:	2	Class	CONFIDENTIAL	Page:	11

(corresponding to the Field of View of SIMBOL-X), this effect could be quantified in a 1.4% for the MS291. This is of the order of the correction reported in Eqs. 2.1 to 2.3, so we *approximately* include it in calculations as follows, where θ is the off-axis angle:

$$V_{286}(E) = 0.1 + 8.50 \tan \vartheta + (0.019 - 8.50 \tan \vartheta) \times (1 - T_{Al}(E)) \quad (2.4)$$

$$V_{291}(E) = 0.1 + 8.35 \tan \vartheta + (0.017 - 8.35 \tan \vartheta) \times (1 - T_{Al}(E)) \quad (2.5)$$

$$V_{295}(E) = 0.1 + 8.24 \tan \vartheta + (0.015 - 8.24 \tan \vartheta) \times (1 - T_{Al}(E)) . \quad (2.6)$$

- 3) *Mirror shell mutual vignetting*: the close spacing between the shells might cause them to be obstructed. In particular, the source divergence causes the MS291 to obstruct a small area of the MS295 when the off-axis angle becomes larger than

$$\vartheta_{obst} = \frac{R_{med}(295) - R_{max}(291)}{L} - \delta = 0.1 \text{ deg} , \quad (2.7)$$

as can be easily derived from data reported in Tab. 1 to Tab. 3. However, if the shells are misaligned by even 0.1 mm, this limit could be even lowered to 4.8 arcmin. Therefore we can expect some vignetting for off-axis angles > 5 arcmin.

The expected on-axis (including a 30 arcsec misalignment of shells wrt. the axis) and an off-axis EA curve are plotted in Fig. 2, for a fixed mirror roughness of 4 Å. The mirror parameters adopted are those listed in Tab. 1 to Tab. 3, the multilayer is described in Tab. 4. Apparently, no EA changes can be expected below 10 keV as long as the off-axis is below 0.1 deg. At higher energies, instead, there is an apparent “smoothing” of reflectivity also below that limit.

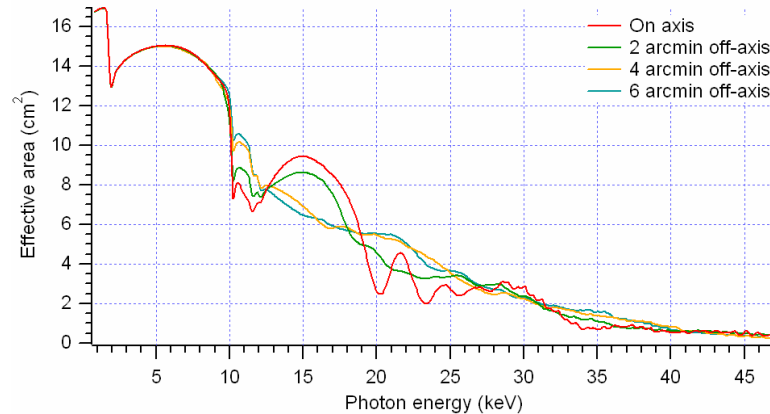



Fig. 2: Theoretical on-axis and off-axis effective area simulations for the entire EM#3 optic. The roughness has been fixed at 4 Å, W density at 17.5 g/cm³.

It is worth noting that, only for an incidence angle larger than 0.27 deg (see Tab. 1 to Tab. 3) some part of the outer surface of mirror shells is exposed to direct X-ray flux, then some beam could in principle reach the detector after bouncing back and forth between the shells, reflected alternatively by the optical and the NiCo surface. Unfortunately, for off-axis angles larger than 0.15 deg the single-reflection coroneae cross the focal spot and no measurement will then be possible.

		X-ray tests at PANTER on Nickel-Cobalt EM#3 (phase A) SIMBOL-X optic prototype						
Code:01/2009	INAF/OAB Technical Report	Issue:	2	Class	CONFIDENTIAL	Page:	12	

3. System alignment and best foci

Like in previous tests [AD2, AD3, AD4], the alignment of the optic to the X-ray beam was driven by motors, able to rotate (horizontally) and tilt (vertically) the jig. The positions of the optic could be monitored along with two encoders, returning continuously the rotation and tilt angles of the system (an encoder step equals an arcsec rotation). The best alignment to the source is obtained by centring the focal spot in the center of the single-reflection coronae. In spite of the large diameter (8 cm) of the PSPC, however, it was impossible to observe all the coronae (~ 5 cm radii, see Tab. 1 to Tab. 3) with a single exposure, therefore it was necessary to move the PSPC off-center, at 4 different lateral positions. The coronae, obtained with a “mosaic” of single PSPC exposures (Fig. 3), enable the alignment evaluation a posteriori (and to correct it if needed). Though they are confocal, the three shells cannot be exactly aligned coaxially, hence their best-align position will be different in general, and the coronae will not be concentric (Fig. 3).

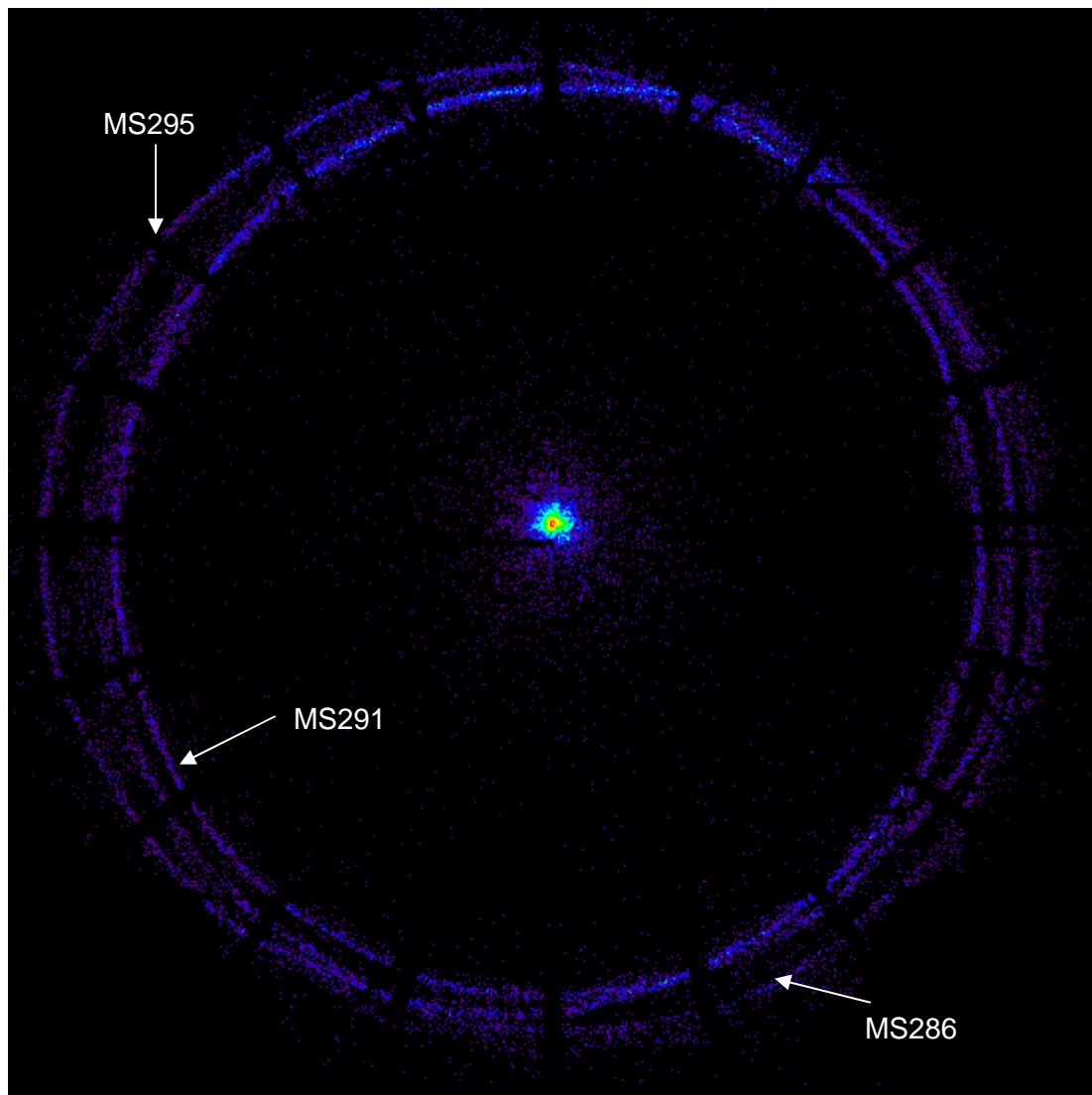



Fig. 3: A mosaic of PSPC images of focal spot and single-reflection coronae of the EM#3 at 1.49 keV.

	X-ray tests at PANTER on Nickel-Cobalt EM#3 (phase A) SIMBOL-X optic prototype					
Code:01/2009	INAF/OAB Technical Report	Issue:	2	Class	CONFIDENTIAL	Page: 13

From Fig. 3 the accurate alignment positions of the 3 shells could be computed. By averaging them, a 17 vertical misalignment of the overall EM#3 could be derived. After the correction of this misalignment, the orientations of the 3 shells with respect to the best align of the EM#3 are listed in Tab. 5. It is seen that the misalignment of shells wrt. the adopted position does not exceed 30 arcsec, with little influence on the effective area. For the measurements of the single MS286 its best alignment position was selected. When more than one shell was measured at the same time (e.g. MS291+MS295), the average of the best-alignment angles was selected. In any case, the small misalignment of shell was accounted for in the computation of the model EA. For the off-axis (at 2, 4, 5 arcmin) measurements, the rotation will be referred to the EM#3 axis and the small misalignments were accounted for in the EA models.

Tab. 5: Approximate (± 5 arcsec) alignment positions of the 3 mirror shells, referred to the adopted alignment of EM#3. The + sign in the horizontal rotation corresponds to the off-axis direction used in the measurements.

Rotation	MS286	MS291	MS295	291+295	EM#3
Horizontal (arcsec)	-17	-22	+38	+8	0
Vertical (arcsec)	-5	+10	-5	+3	0
Total (arcsec)	18	24	38	9	0

Also the focal lengths of the shell are not identical (Sect. 2.1). The focal distances, relative to the source at finite distance (120.90 m), have been measured by finding the detector position along the axis that minimizes the HEW, in correspondence to the vertices of the parabola. Fig. 4 reports the results and shows that the focal plane of the MS286 is located at a 10.997 m distance from the intersection plane and that of the pair MS291+MS295 at 10.962 m. For the whole EM#3 the focus is 10.976 m behind the intersection plane. A 5 mm error can be assumed on these quotes.

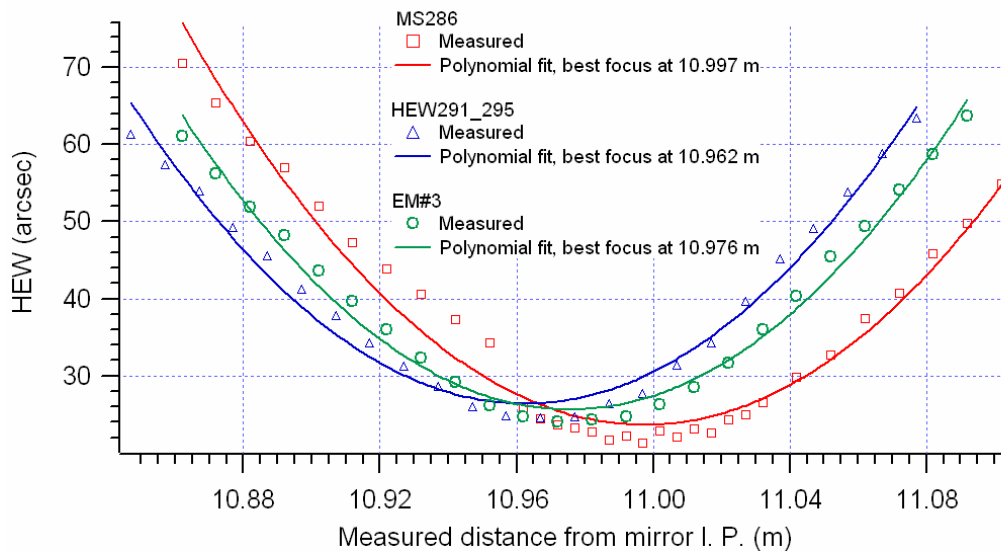



Fig. 4: The HEW (measured with the PSPC at 1.49 keV) of the two mirror shells as a function of the detector position along the axis. The vertices of the best parabolic fits locate the focal planes. The HEW were computed over the whole PSPC field.

	X-ray tests at PANTER on Nickel-Cobalt EM#3 (phase A) SIMBOL-X optic prototype						
Code:01/2009	INAF/OAB Technical Report	Issue:	2	Class	CONFIDENTIAL	Page:	14

We can now derive, from the measured focal positions f' , the true focal lengths f , using the formula (see e.g. [RD3]):

$$f = \frac{f'D}{D + f'} \quad (3.1)$$

where $D \approx 120.90$ m is the source distance. We also estimate the relative error on f :

$$\varepsilon_f^2 = \frac{D^2}{(D + f')^2} \varepsilon_{f'}^2 + \frac{f'^2}{(D + f')^2} \varepsilon_D^2; \quad (3.2)$$

as $D \approx 10f'$, f is 10 times less sensitive to an error on D than on f' . This means that an error of 1 cm on D translates into a 1 mm error on f , much less than the error introduced by f' . So we get

$$f_{286} = (10.07 \pm 0.01) \text{ m} \quad \text{and} \quad f_{291+295} = (10.05 \pm 0.01) \text{ m}; \quad (3.3)$$


the best focus of the whole EM#3 optic (green points and line in Fig. 4) is – as expected – intermediate between the other two. The focal distance for a source at infinity can be calculated with the Eq. (3.1), yielding

$$f_{\text{EM\#3}} = (10.06 \pm 0.01) \text{ m}, \quad (3.4)$$

exactly in the middle of the two. We can now use this number to determine the focal lengths for a source at infinity, as measured with the Brera VOB, for all the shells using the reported values in Tab. 1 to Tab. 3. The found values for the absolute focal lengths match well the diameters and the incidence angles on the shells.

The HEWs at the best foci (at 1.49 keV) deserve a few words. For the MS286 it is ~ 21 arcsec (over all the PSPC field), in good agreement with the measurement at the VOB (Tab. 1). Notice that this is slightly larger than the values reported in the next section, due to the smaller ROI adopted there – to allow the comparison with TRoPIC. For the MS291+MS295 it is 24.5 arcsec, larger than the measured ones with the two shells, separately (24 and 19 arcsec with the VOB). This is due, expectedly, to the difference in focal length. The resulting focal length is close to that of the MS295, whereas the MS291 that is *defocused by 2 cm, resulting in a 13 arcsec additional HEW* (following [RD4]). Summation in quadrature for the defocused MS291 yields 27.3 arcsec. Finally, averaging with the HEW of the MS295 (at the best focus) returns 23.2 arcsec, vs. 24.5 measured at PANTER. The average is justified by the similar areas of the two shells.

Similar comments apply to the EM#3. Defocusing the three MS286, MS291, MS295 by 1,3,1 cm respectively we obtain 22.7 arcsec as average HEW, vs. the measured 24 arcsec. The agreement is quite good, considering the uncertainties on the focal length and on the HEW of the shells as measured with the VOB.

	X-ray tests at PANTER on Nickel-Cobalt EM#3 (phase A) SIMBOL-X optic prototype						
Code:01/2009	INAF/OAB Technical Report	Issue:	2	Class	CONFIDENTIAL	Page:	15

4. Mirror shell 286

4.1. The PSPC and TRoPIC views

The focal spot of the MS286 at low energies, as seen with the PSPC detector at 0.93 keV photon energy, is displayed in focus and intra-focus in Fig. 5. This is the minimum energy used in the measurement campaign, that should also minimize the impact of the X-ray scattering on the HEW. *All the images here reported span over a 360 arcsec angular diameter*, even though the full PSPC field would be much larger. This selection has been done to ease the comparison with TRoPIC. The intra-focus image is a symmetric ring, clearly modulated into 20 segments due to the spider spokes shading. A faint central spot, related to a concentration of scattered rays in the common intersection of the planes of incidence onto the mirror, is also visible in the intra-focal image. The integration time for each exposure, though variable from case to case, was in the range 5-10 min, sufficient to record a photon count rate with a 0.5-1% accuracy, for flat fields, for in-focus and OOF exposures.

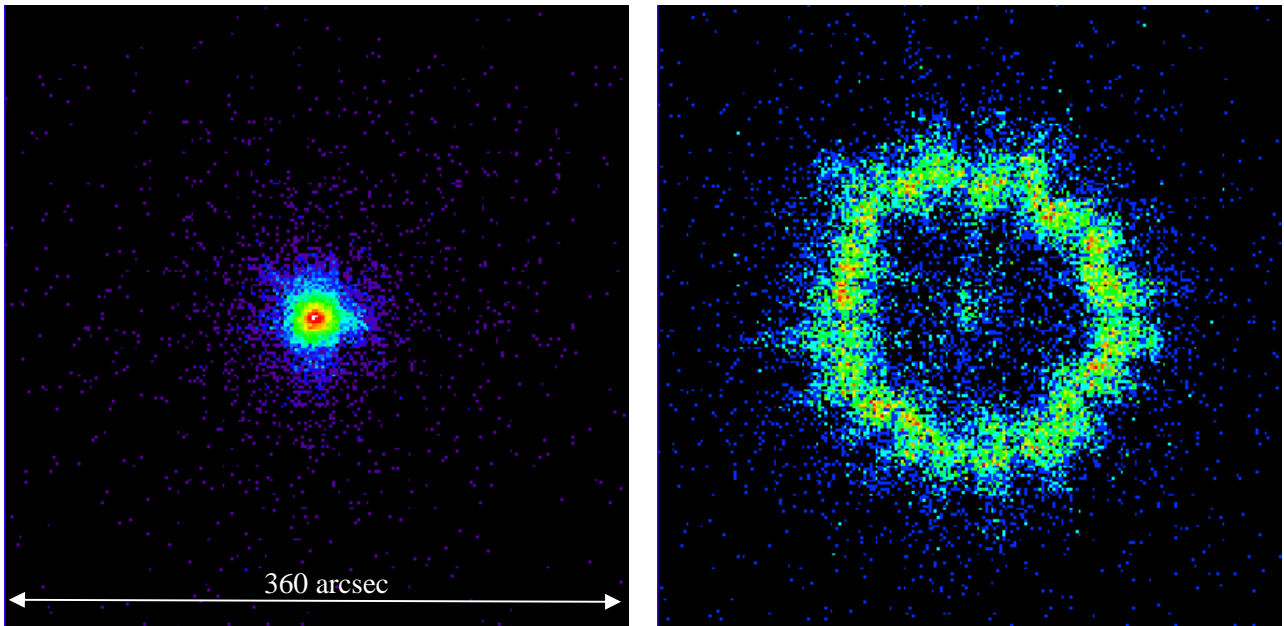



Fig. 5: the on-axis focal spot of the MS 286 at 0.93 keV (the Cu-La line), as seen by the PSPC. Logarithmic colour scale. (left) in focus, (right), 35 cm intra-focal.

The in-focus HEW of the MS286 at 0.93 keV, computed over a ROI with radius 180 arcsec, is **18.2 arcsec**. This value can mainly be assumed as an estimation of the figure error of the mirror shell and the errors introduced at the integration stage. This also falls in proximity of the result obtained with the VOB (Tab. 1). This HEW value is only loosely dependent on the considered ROI: e.g., extending the calculation to all the PSPC field, the resulting HEW would be larger by ~ 1 arcsec. In the following we will always refer to a 180 arcsec radius ROI also for the PSPC, for consistency with TRoPIC, that covers exactly a 360 arcsec angular diameter when seen from a 11 m distance. More HEW values at different photon energies for the MS286 can be found in Sect. 4.3.

In Fig. 6 we display some PSPC images of the focal spot of the MS286 at 0.93 keV, after *tilting horizontally the optic by 4 arcmin*, in order to simulate a 4 arcmin off-axis source. The image sizes are the same as Fig. 5, with the detector position unchanged.

	X-ray tests at PANTER on Nickel-Cobalt EM#3 (phase A) SIMBOL-X optic prototype						
Code:01/2009	INAF/OAB Technical Report	Issue:	2	Class	CONFIDENTIAL	Page:	16

At a glance, the in-focus, off-axis focal spot (Fig. 6, left) is essentially indistinguishable from the in-focus image on-axis (Fig. 5, left). Both are quite symmetric and, by computing the HEW of the off-axis focal spot in focus (i.e. at the best focus of the on-axis exposure), one obtains **19.1 arcsec** (always within a 180 arcsec radius ROI), only slightly larger than the corresponding HEW on-axis. This effect is systematic, i.e. it can be observed at all photon energies (see

Tab. 6). However, the HEW at 5 arcmin off-axis is in general smaller than the corresponding values at 4 arcmin off-axis, suggesting a diminishing impact of X-ray scattering as the off-axis angle is increased.

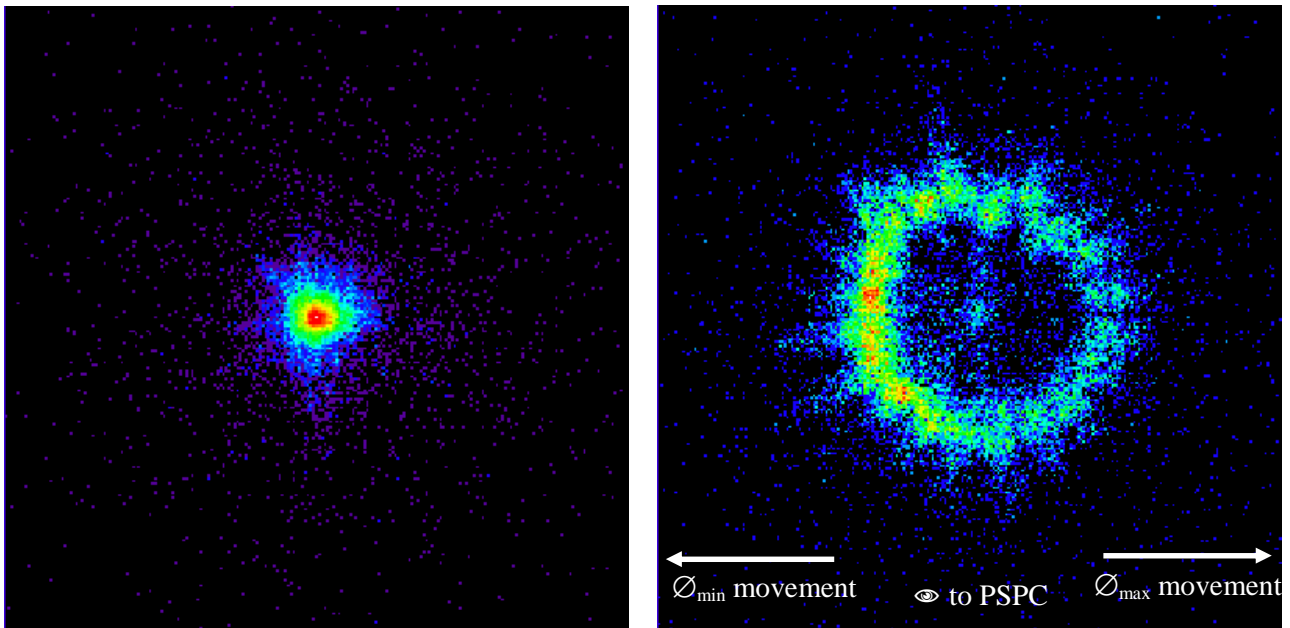



Fig. 6: 4 arcmin off-axis focal spot of the MS 286 at 0.93 keV (the Cu-La line), as seen by the PSPC. Logarithmic colour scale. In the image reference frame, the optic is rotated about the vertical axis, in counter-clockwise sense for an observer placed atop. (left) in focus, (right), 35 cm intra-focal. Not shown is the single-reflection corona, that falls in the right part of the PSPC field.

On the contrary, the intra-focal image of the MS286 in off-axis setup (Fig. 6, right) differs significantly from the on-axis one (Fig. 5, left). The off-axis image exhibits a clear asymmetry, as the sectors on the left side reflect much better. This is caused by the variation of the incidence angles on the mirror, depending on the azimuthal coordinate of impact. In particular, the sectors on the left offer a larger cross-section to X-rays (even though at first glance the contrary would seem more intuitive). In fact, in mirror sectors at left the geometrical vignetting for double reflection [RD3] is reduced as the incidence angles on the parabola and the hyperbola become more similar, at the expense of the sectors on the right side. In fact, we see that the effective area *at low energies* (i.e. below 10 keV) remains essentially unchanged with respect to the on-axis case (see Sect. 4.2), in agreement with the theoretical model (see Fig. 2).

An in-focus and an out-of focus, on-axis image of the MS286 focal spot, obtained with TRoPIC up to 50 keV, are displayed in Fig. 7. The in-focus image does not significantly exhibit relevant features (even if the image is better resolved than with the PSPC), but an apparently larger amount of scattering in the TRoPIC field. This becomes also apparent from the OOF image: in fact,

	X-ray tests at PANTER on Nickel-Cobalt EM#3 (phase A) SIMBOL-X optic prototype						
Code:01/2009	INAF/OAB Technical Report	Issue:	2	Class	CONFIDENTIAL	Page:	17

the central spot, caused by the concentration of XRS, is much more evident than at low energies (Fig. 5), and it becomes even the point with maximum count rate throughout the image. On the contrary, as in the 0.93 keV exposure the maximum was spread over the “ring”.

The optic was tested in energy-dispersive setup with TRoPIC and the X-ray source at 20, 35 and 50 kV voltage. At low energies, the reflectivity of the mirror is expectedly larger, hence the risk of pileup occurrence is larger in the 20 kV setup, and chiefly in the central pixels where the maximum concentration of photons takes place. The anode current was then lower for the in-focus exposures (2 mA at 20 to 35 kV, and 5 mA at 50 kV), and higher for the OOF ones (8 mA at 20 and 50 kV, 15 mA at 35 kV). Note that the focus is slightly off-center in the images. The X-ray beam was attenuated by interposition of Ti filters with variable thickness: at 20 kV, 300 μm for the Flat Fields and the intra-focal images and 500 μm for the in-focus images; at 35 kV, a 1 mm thick Ti filter for all exposures; at 50 kV, a 1 mm Ti filter and the “V20” window kept closed to act as a further filter. The adopted preventive measures allowed to keep the pileup rate below 0.5% in the in-focus images, and even below 0.2% in the OOF exposures (uniformly-distributed over the ring). The integration times used with TRoPIC have been, in general, 1 h for out-of focus measurements and 40 min for in-focus exposures.

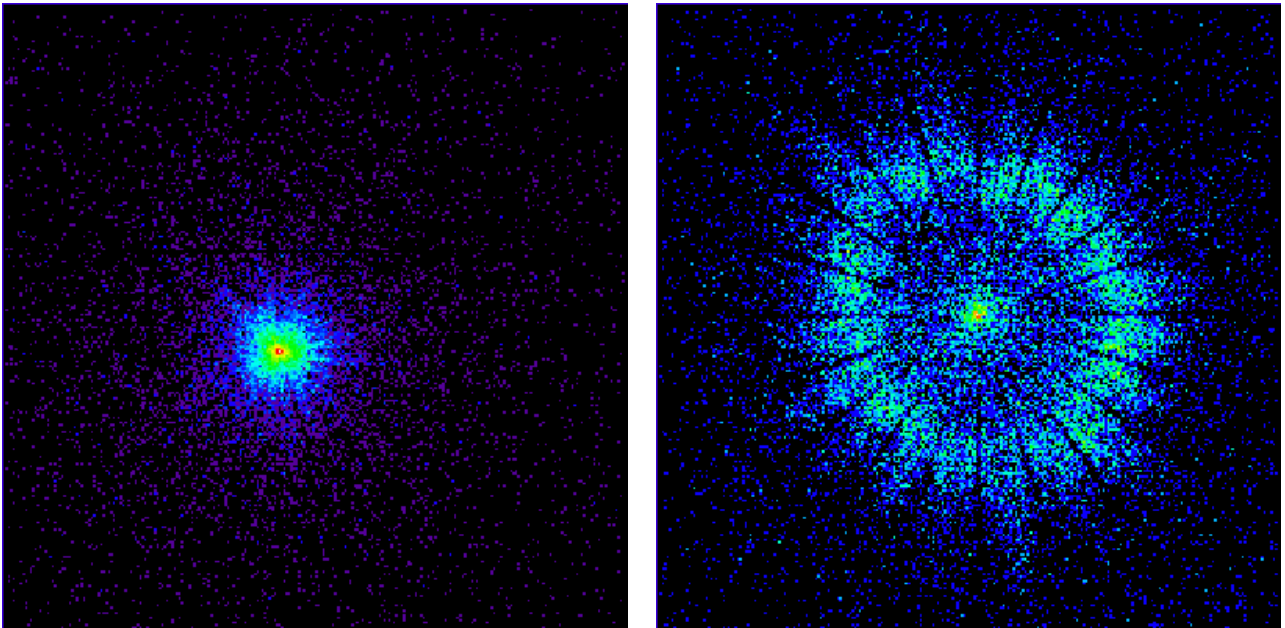



Fig. 7: on-axis focal spot of the MS286 as seen by TRoPIC, with the X-ray source at 50 kV setup. Logarithmic colour scale. (left) in focus, (right), 35 cm intra-focal.

4.2. Effective areas

EA values of the MS286 are obtained from the integration of the images to obtain the total count rate (spectrally-resolved for the measurements with TRoPIC). The count rate has then been normalized to the count rate per unit area of the incident beam, using the Flat Field exposure. Actually, as the Flat Field image (2 cm diam. + beam divergence) did not fit into the TRoPIC field (19.2 mm wide), a 200×200 pixel rectangle was selected in each Flat Field to probe the incident beam. The incident beam density was then obtained by normalization to the 200×200 pixel area,

	X-ray tests at PANTER on Nickel-Cobalt EM#3 (phase A) SIMBOL-X optic prototype						
Code:01/2009	INAF/OAB Technical Report	Issue:	2	Class	CONFIDENTIAL	Page:	18

that translates into an equivalent area of 1.89 cm² at the optic location. We always adopted a 180 arcsec radius ROI to execute the focal spot integration, for both PSPC and TRoPIC.

4.2.1. On-axis EA

As pileup is not an issue for the PSPC, the measured EA values at the *monochromatic* energies from 0.93 to 8.045 keV, have been obtained from *in-focus PSPC images*. The results are plotted in Fig. 8 (circles), overplotted to the expected effective area curves. Theoretical models are obtained along with the reflectivity computed from the multilayer parameters of Tab. 4, for different surface roughness values. Below 10 keV, the measured values lie well on the theoretical curves: this confirms that the X-ray flux is properly impinging on the mirror. In this energy range, roughness is almost of no influence on the reflectivity in this energy range, as it can be seen from the degeneracy of theoretical models below 10 keV. Moreover, no guess is provided by experimental data regarding the multilayer structure, as the photon reflection occurs in total reflection regime. The statistical error on the measured effective area is close to 1%.

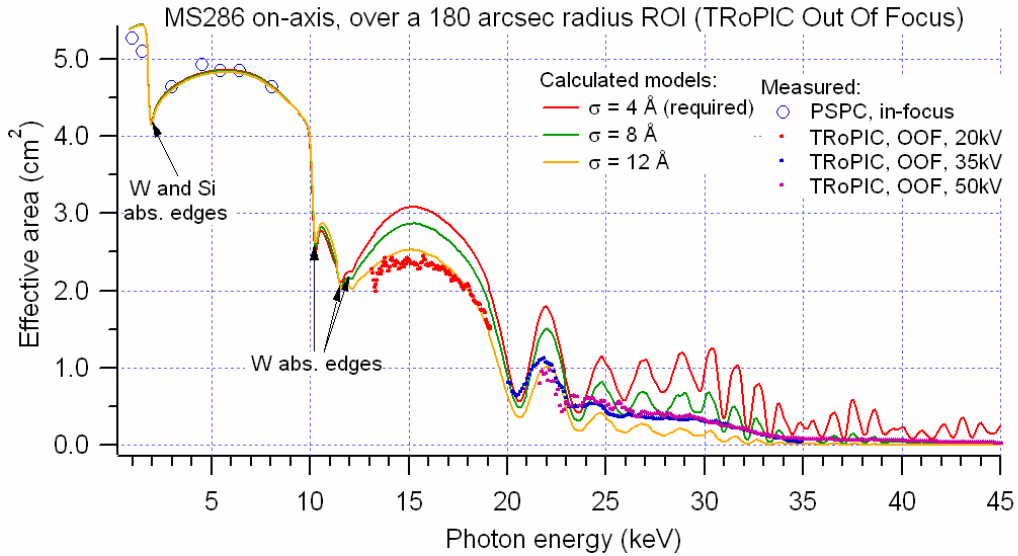



Fig. 8: the on-axis effective areas for the MS286, as measured with the PSPC in monochromatic setup, and with TRoPIC in energy-dispersive setup, from OOF images. Error bars in the EA data are omitted for clarity, but the statistical error is in general of a few percent.

High-energy (> 10 keV) data have been *firstly* obtained with TRoPIC *from the OOF images*, in energy-dispersive setup (Fig. 8, dots). This has been done in order to minimize the risk of pileup occurrence, hence to increase the X-ray source power, abridging the integration time. This allowed the statistical error of the EA measurement to be fairly low: 3% at 18 keV, 4% at 30 keV, 11% at 40 keV. We see that the measured EA values are qualitatively in agreement with the model, even if the measured reflectivity is systematically below the theoretical predictions and, in particular, with respect to the model with 4 Å rms roughness, which corresponds to the theoretical requirement. We see, instead, that the measured EA values match better the curve with 8 Å, and even 12 Å below 20 keV.

In-focus TRoPIC images were also processed to check the results of Fig. 8, as also for them the pileup was kept at a very low level using a thicker filter and a lower current than for OOF

		X-ray tests at PANTER on Nickel-Cobalt EM#3 (phase A) SIMBOL-X optic prototype						
Code:01/2009	INAF/OAB Technical Report	Issue:	2	Class	CONFIDENTIAL	Page:	19	

images (Sect. 4.1). The computation of the EA accounted for the different current used for the Flat Fields and the in-focus measurements, and for the photo-absorption from the different Ti filters used as beam attenuators. The results of the in-focus measurement are plotted in Fig. 9. In general, due to the much lower count rate of the in-focus image, the statistical error will be larger than for OOF measurements: 10% at 18 keV, 8% at 30 keV, 15% at 40 keV. This is the reason why in-focus measurements were not considered for computing the EAs in previous campaigns [AD2, AD3, AD4].

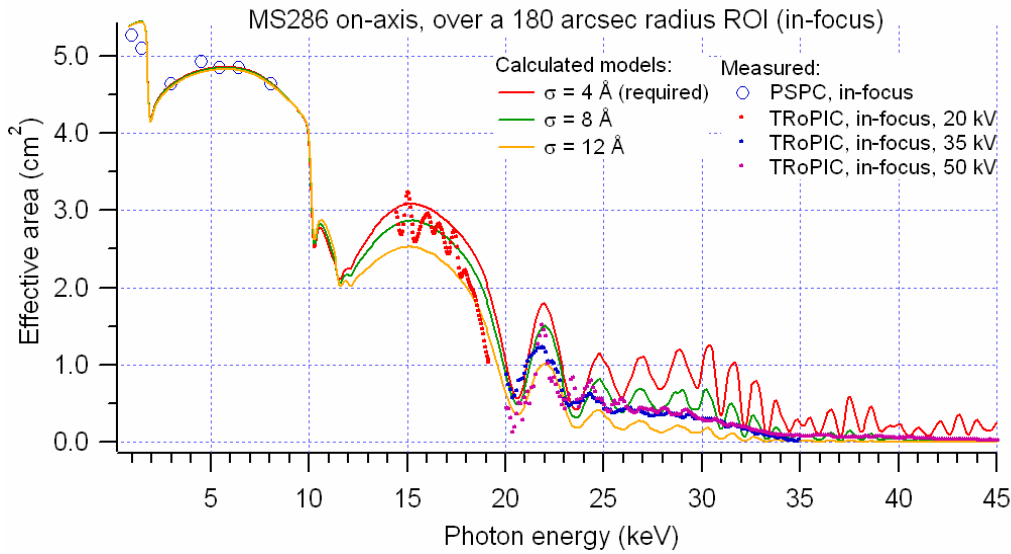



Fig. 9: the on-axis effective areas for the MS286, as measured with the PSPC in monochromatic setup, and with TROPIC in energy-dispersive setup, from in-focus images. Though omitted for clarity, error bars are larger than 10%.

The comparison shows that there is a sensitive EA gain for the in-focus setup (20% at 18 keV) up to 25 keV, while beyond this energy the measured EA values are very similar. In fact, the in-focus EAs are more consistent with the theoretical model assuming a 8 Å roughness, whilst the EAs OOF matched better a 12 Å below 25 keV (Fig. 8). The difference might be related to X-ray scattering, as for OOF images the ring is close to the detector's edge and several photons may have been scattered out of its field.

In practice, the OOF results (Fig. 8) represent the EA of the MS286, as measured over a smaller ROI due to the closeness of TROPIC edge. The effect may be, indeed, reduced beyond 25 keV, because softer X-rays are scattered at larger scattering angles by a given range of spectral components of surface roughness. The roughness values obtained from experimental data will be compared with metrological data aimed at a direct measurements of mirror surface roughness.

4.2.2. Off-axis EA

Measurements of off-axis EA of the MS286 have been performed with the PSPC in monochromatic setup at 2, 4, 5 arcmin off-axis. In particular, we report in Fig. 10 the effective area *at a 4 arcmin off-axis* (wrt. the best align of EM#3). The effective areas below 10 keV with a 2 or 5 arcmin off-axis are essentially unchanged with respect to the values, reported here, for 4 arcmin off-axis. The measured EA values (within a 1% error) are compared in Fig. 10 with the theoretical models,

	X-ray tests at PANTER on Nickel-Cobalt EM#3 (phase A) SIMBOL-X optic prototype						
Code:01/2009	INAF/OAB Technical Report	Issue:	2	Class	CONFIDENTIAL	Page:	20

assuming different roughness values of the mirror surface; the misalignment reported in Tab. 5 was added to the off-axis in the computation of models.

Below 10 keV, the EA measured values match very well the theoretical curves (with the exception of the 0.93 keV photon energy). No data are available beyond this energy. Notice that the EA values are almost unchanged with respect to the on-axis case, and do not allow to retrieve information on surface roughness.

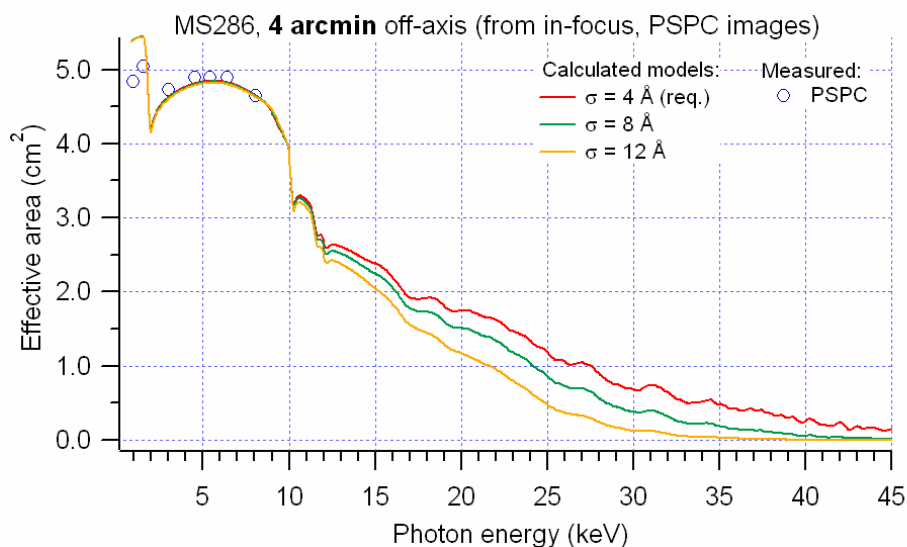



Fig. 10: 4 arcmin off-axis effective areas for the MS286, as measured with the PSPC in monochromatic setup.

4.3. HEW and W90

The HEW values of the MS286, as measured with the PSPC as a function of the energy below 10 keV (Tab. 6), exhibit an increasing, on- and off-axis, trend due to the increasing relevance of the X-ray scattering with the photon energy, even if the HEW is still dominated by figure errors. The HEW, below 10 keV, changes very slowly with the off-axis angle. The off-axis was limited to 5 arcmin to avoid a contamination from the single-reflection corona, that would enter the ROI for higher off-axis.

Tab. 6: on-axis and off-axis HEW (± 0.2 arcsec) of the MS286 at low energies (ROI < 180 arcsec).

HEW (arcsec)	Cu-L α (0.93 keV)	Al-K α (1.49 keV)	Ag-L α (2.98 keV)	Ti-K α (4.51 keV)	Cr-K α (5.41 keV)	Fe-K α (6.40 keV)	Cu-K α (8.05 keV)
on-axis	18.2	18.5	20.1	21.8	22.0	22.5	23.3
2 arcmin off-axis	18.4	18.8	21.3	21.4	23.2	22.8	24.0
4 arcmin off-axis	19.1	19.6	21.2	23.1	22.9	23.2	24.9
5 arcmin off-axis	18.2	19.0	21.9	22.3	22.2	22.5	23.5

	X-ray tests at PANTER on Nickel-Cobalt EM#3 (phase A) SIMBOL-X optic prototype						
Code:01/2009	INAF/OAB Technical Report	Issue:	2	Class	CONFIDENTIAL	Page:	21

The systematically-larger values of the HEW off-axis, with respect to the on-axis values, might in principle be related to optical aberrations like *coma* and *field curvature*. Quantification of these effect can be done along with the empirical formulae reported in [AD7]: application to our specific case returns a theoretically-predicted focal spot blur reported in the first column of Tab. 7. The results are given in terms of $\text{FWHM} = 2.345\sigma$, after approximating the mirror PSF with a Gaussian profile of rms σ , and assuming (very roughly) $\text{HEW} \approx \text{FWHM}$. The theoretically-computed aberration was then added in quadrature to the measured HEW on-axis at 0.93 keV, and compared with the experimental off-axis HEW values at the same energy (2nd and 3rd columns of Tab. 7). The agreement is poor, i.e. the invoked aberrations are insufficient to explain the HEW increase as the source is moved off-axis. Moreover, the theory predicts aberrations that increase with the off-axis angle, whereas at 5 arcmin the HEW value is smaller than the one with a 4 arcmin off-axis, at the same photon energy. This is systematically observed at all energies (see Tab. 6), with almost no exceptions.

The W90 measured values at the same energies with the PSPC, always within a 180 arcsec radius, are reported in Tab. 8. Like for the HEW (Tab. 6), also the W90 values with a 5 arcmin off-axis are smaller than the corresponding ones at a 4 arcmin off-axis.


Tab. 7: comparison of predicted off-axis aberration for the MS286 at 0.93 keV (18.2 arcsec on-axis) and experimental results.

Off-axis	Theoretical aberration (FWHM, arcsec)	On-axis HEW (meas. at 0.93 keV) + theoretical aberration (quadratic sum)	Measured HEW at 0.93 keV (arcsec)
0 arcmin	0	18.2	18.2
2 arcmin	0.6	18.2	18.4
4 arcmin	2.3	18.3	19.1
5 arcmin	3.5	18.5	18.2

Tab. 8: on-axis and off-axis W90 (± 3 arcsec) of the MS286 at low energies ($\text{ROI} < 180$ arcsec).

W90 (arcsec)	Cu-L α (0.93 keV)	Al-K α (1.49 keV)	Ag-L α (2.98 keV)	Ti-K α (4.51 keV)	Cr-K α (5.41 keV)	Fe-K α (6.40 keV)	Cu-K α (8.05 keV)
on-axis	75	84	91	105	104	107	107
2 arcmin off-axis	78	87	93	104	107	103	107
4 arcmin off-axis	86	90	101	115	114	110	113
5 arcmin off-axis	79	88	96	105	108	104	108

The on-axis HEW trend at low and high energies is reported in Fig. 11. The HEW values were measured within a 170 arcsec circle because the focal spot did not fall exactly in the center of TRoPIC field, then the largest circular, centred on the focal spot, ROI that could fit in was only 340 arcsec wide instead of 360. Starting from the initial HEW values at 0.93 keV, the HEW exhibit a typical increasing trend caused by the increasing relevance of the X-ray scattering. It seemingly

		X-ray tests at PANTER on Nickel-Cobalt EM#3 (phase A) SIMBOL-X optic prototype						
Code:01/2009	INAF/OAB Technical Report	Issue:	2	Class	CONFIDENTIAL	Page:	22	

tends to “saturate” up to 20 keV, then starts to increase again, in a nearly-linear fashion. The oscillations in the HEW trend are probably due to the modulation of the X-ray scattering, caused by the interference of scattered X-rays by the roughness of each multilayer interface. In Fig. 27 the experimental HEW trend is compared with that of the MS291+295 and that of the EM#3.

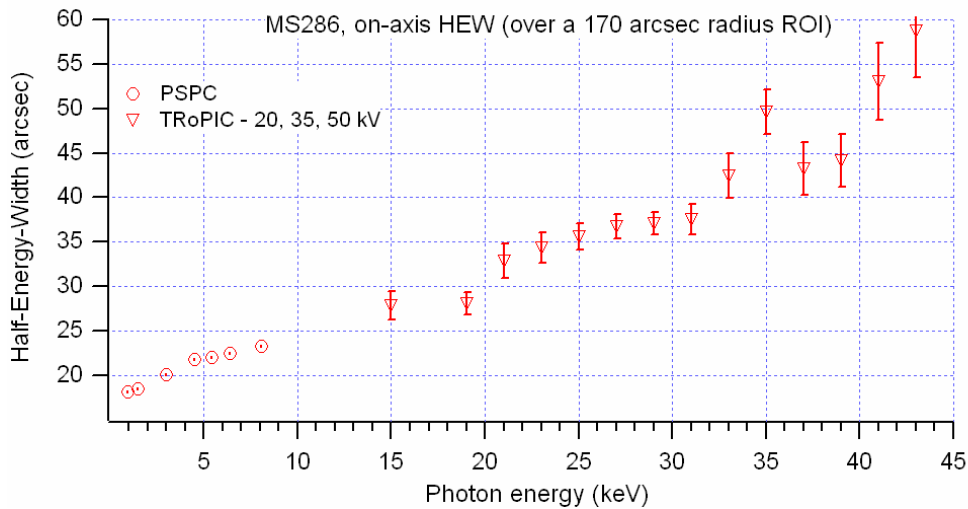



Fig. 11: on-axis HEW values for the MS286, as measured with the PSpC in monochromatic setup (circles) and in energy-dispersive setup with TRoPIC (triangles).

	X-ray tests at PANTER on Nickel-Cobalt EM#3 (phase A) SIMBOL-X optic prototype						
Code:01/2009	INAF/OAB Technical Report	Issue:	2	Class	CONFIDENTIAL	Page:	23

5. Mirror shell 291 and 295

5.1. The PSPC and TRoPIC views

The MS291 and MS295 have been measured together. Some portions of PSPC fields (360 arcsec wide) in monochromatic setup at 0.93 keV are displayed in Fig. 12. With respect to the images of the MS286 (Sect. 4.1), the focal spot is less symmetric; the in-focus image exhibits two spokes at 90°, one of them clearly related to a “bump” in the upper part of all of the OOF images. We have no way, from this dataset, to discriminate which shell is responsible for this defect, but it seems likely that the deformation was arisen at the handling and integration stage, as the optical quality of the MS291 (and the MS286) in UV light was observed to worsen with the respect to that of the free-standing mirror.

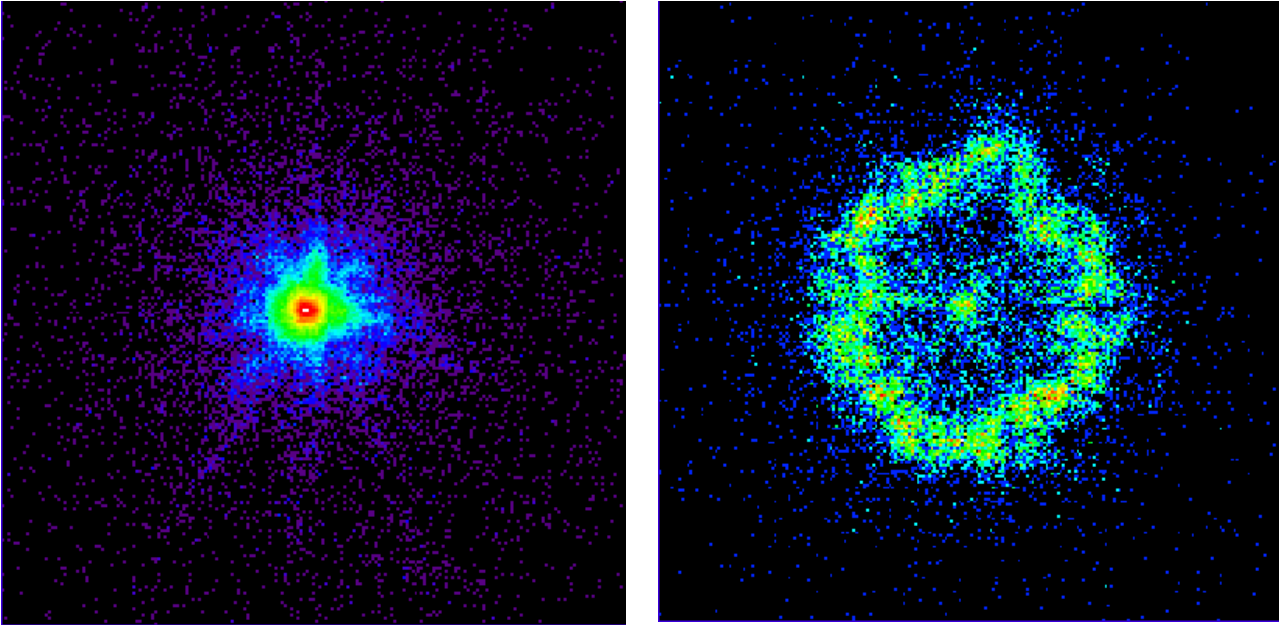



Fig. 12: the on-axis focal spot of the MS291+295 at 0.93 keV (the Cu-La line), as seen by the PSPC. Logarithmic colour scale. (left) in focus, (right), 31.5 cm intra-focal.

The MS291+295 have been tested with the PSPC at the monochromatic energies listed in Tab. 9, on-axis and off-axis by 2, 4, 5 arcmin, in-focus and OOF. The HEW at 0.93 keV, as measured over a 180 arcsec ROI (for consistency with TRoPIC, see Sect. 4.1), is **21.5 arcsec**, better than we got with the previous prototype, the EM#2, made of 2 shells from the same mandrels [AD4], but it should be remembered that the focal lengths of the two shells of the EM#2 differed by 8 cm instead of 2 (Sect. 3). Then the defocusing in the present case is much lower than for the EM#2, and the HEW of the two individual shells are expectedly worse than those of the EM#2 which, at the respective best foci, had 15-16 arcsec HEW.

In Fig. 13 we display two images at 0.93 keV for a 4 arcmin off-axis. The tilt direction of the optic is the same of Fig. 6. The off-axis is responsible for the asymmetry in the OOF image (Sect. 4.1). The integration times have been shorter (2 to 5 minutes) than for the MS286 due to the larger EA of the two MS together, in order to keep the same statistical error on the count rates (between 0.5 and 1%).

	X-ray tests at PANTER on Nickel-Cobalt EM#3 (phase A) SIMBOL-X optic prototype						
Code:01/2009	INAF/OAB Technical Report	Issue:	2	Class	CONFIDENTIAL	Page:	24

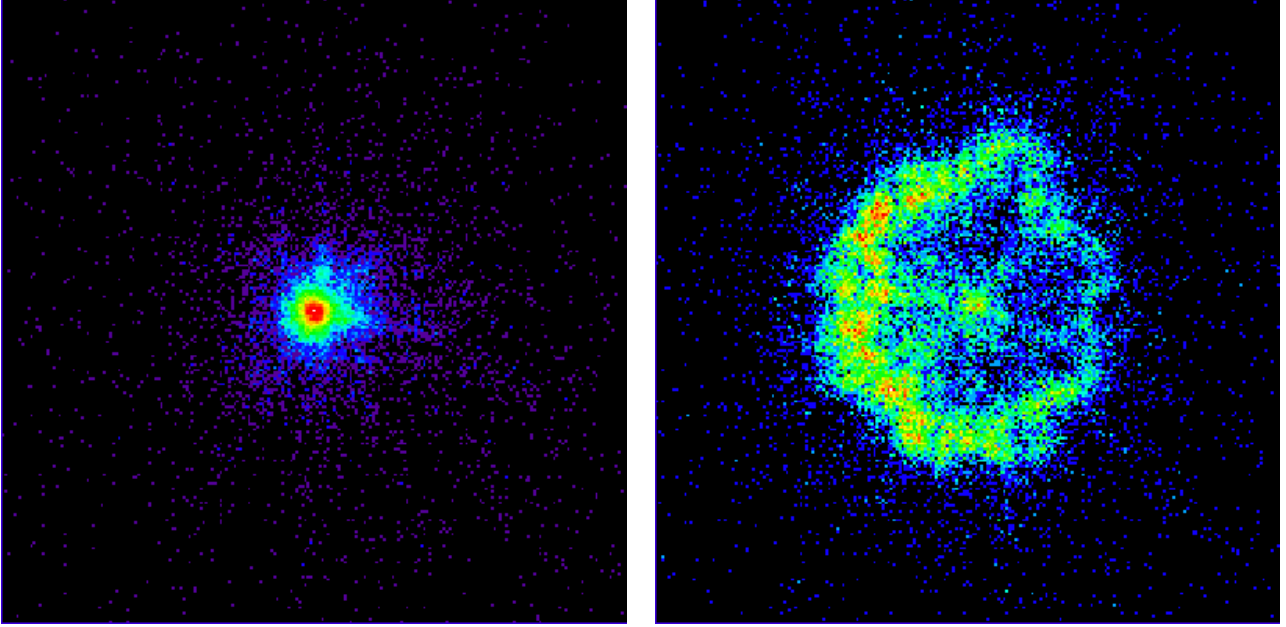


Fig. 13: 4 arcmin off-axis focal spot of the MS291+295 at 0.93 keV (the Cu-La line), as seen by the PSPC. Logarithmic colour scale. (left) in focus, (right), 31.5 cm intra-focal.

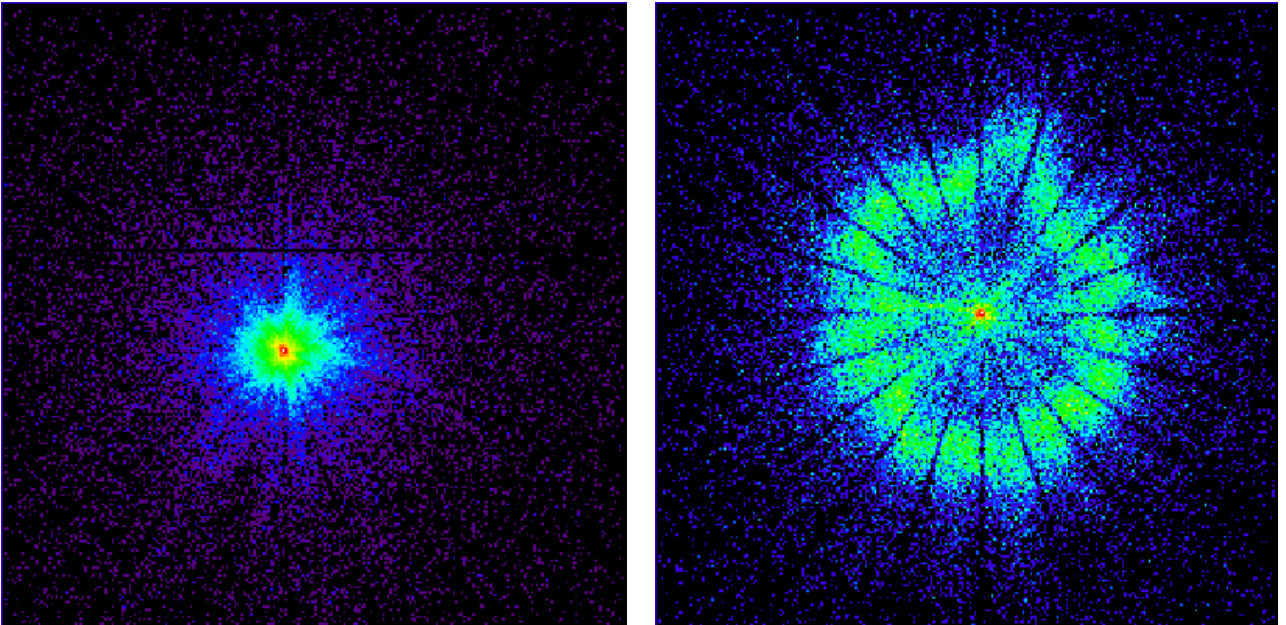



Fig. 14: on-axis focal spot of the MS291+295 at seen by TRoPIC, with the X-ray source at 50 keV setup. Logarithmic colour scale. (left) in focus, (right), 31.5 cm intra-focal.

In Fig. 14 we plot a TRoPIC field with the source at 50 keV setup, i.e. illuminated by a continuum X-ray spectrum up to 50 keV. The amount of X-ray scattering in the TroPIC field, responsible for the HEW increase and the Effective Area loss, is clearly visible in both in-focus and intra-focal image. Notice also the major relevance of the central spot in the OOF image, with respect to the low-energy measurements (Fig. 12 and Fig. 13). The X-ray source settings and the

	X-ray tests at PANTER on Nickel-Cobalt EM#3 (phase A) SIMBOL-X optic prototype						
Code:01/2009	INAF/OAB Technical Report	Issue:	2	Class	CONFIDENTIAL	Page:	25

integration times have been the same used to test the MS286 (Sect. 4.1). Even if the larger effective area could have increased the risk of pileup, it turned out to be very low in the in-focus images (less than 0.4% at 20 kV, where the reflectivity is the highest). In the OOF images, paradoxically, the same pileup percent is present as the source power was increased. Moreover, most pileup occurs in the central spot also in the OOF image (Fig. 14, right).

5.2. Effective areas

5.2.1. On-axis EA

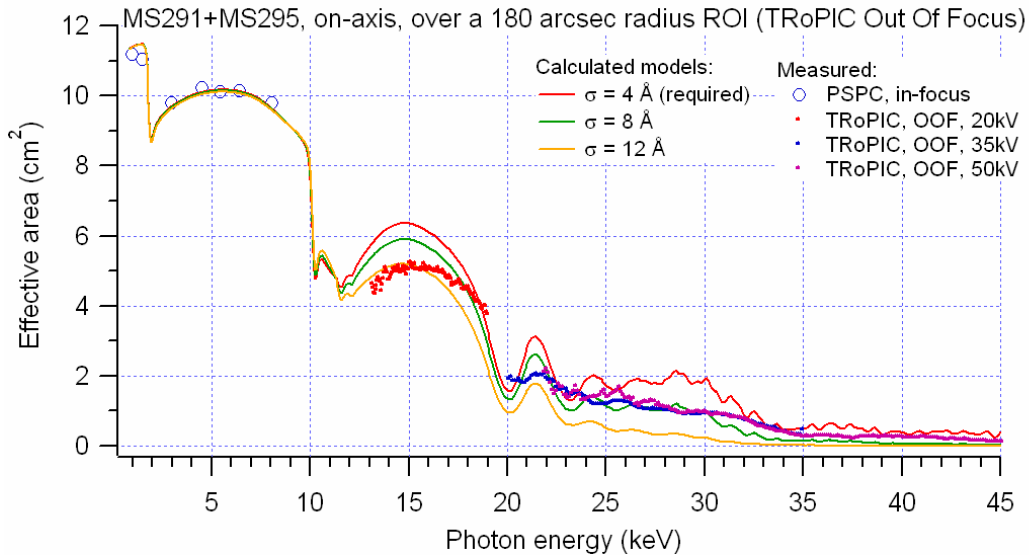



Fig. 15: the on-axis effective areas for the MS291+295, as measured with the PSpC in monochromatic setup, and with TRoPIC in energy-dispersive setup, derived from the OOF exposures.

For the EAs measured *on-axis* for the MS291+295, similar comments apply as those for the MS286 (Sect. 4.2.1). The EA values at low energies (below 10 keV), as measured with the PSpC within 1%, match very well the theoretical predictions (Fig. 15), regardless of the surface roughness since models with very different σ return almost the same predictions.

At higher energies (beyond 10 keV) the measured EA with TRoPIC, *out-of-focus*, matches the prediction qualitatively, but it is considerably below the required EA values, i.e. the curve with a 4 Å surface roughness (Fig. 15). In this case the high flux allowed by the OOF setup allowed a good statistics (the error on the EA values is 2.5% at 18 keV, 2% at 30 keV, 7% at 40 keV).

The results of EA measurements with TRoPIC *in-focus* are displayed in Fig. 16. The situation looks very similar to that of MS286 (Sect. 4.2.1), with an in-focus measurement characterized by a much worse accuracy (6.5% at 18 keV) due to the lower count rate, but with measured effective areas higher than those measured out-of-focus: in fact, *the EA values in-focus up to 20 keV are consistent with the theoretical model assuming 4 Å*. No relevant change is observed instead beyond this energy: at 30 keV the data match a 8 Å also for the in-focus exposures, while around 40 keV the EA is close again to match a model with surface roughness close to 5-6 Å. Details regarding surface roughness, to be investigated along with metrological measurements on mirror samples, are expected to shed light on the interpretation of results.

	X-ray tests at PANTER on Nickel-Cobalt EM#3 (phase A) SIMBOL-X optic prototype						
Code:01/2009	INAF/OAB Technical Report	Issue:	2	Class	CONFIDENTIAL	Page:	26

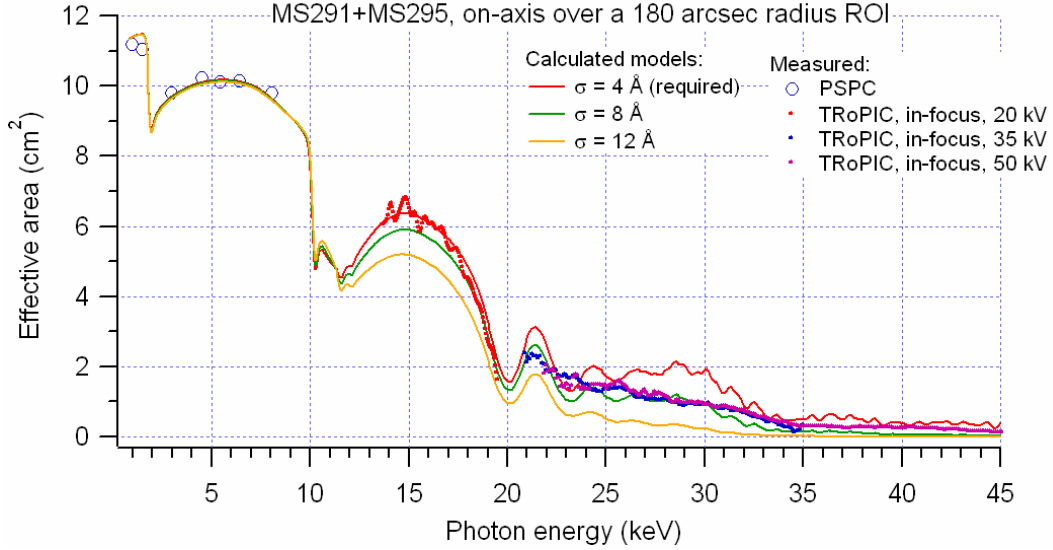


Fig. 16: the on-axis effective areas for the MS291+295, as measured with the PSpC in monochromatic setup, and with TRoPIC in energy-dispersive setup, derived from the in-focus exposures.

5.2.2. Off-axis EA

In Fig. 17 we plot the measured (within a few %) EA values of the MS291+295 off-axis by 4 arcmin, in monochromatic setup. Like for the MS286 (Sect. 5.2.2), the measured EA values match well the predictions. Moreover, their values are almost unchanged with respect to the EA on-axis. The same comments apply for the measured EA at a 2 arcmin off-axis, not shown here. The low-energy EA values at 5 arcmin off-axis are only slightly (a few %) lower than the theoretical estimate due to a small probable obstruction of the MS295 from the edge of the MS291, caused by their mutual small misalignment (see Sect. 2.3 and 3) nearly along the off-axis tilt direction. Probably such an obstruction would not have been seen with an off-axis at -5 arcmin.

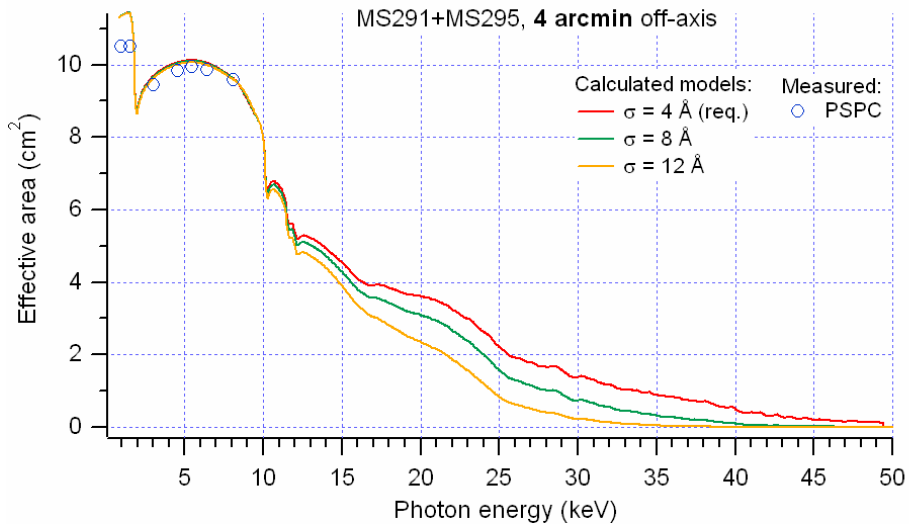



Fig. 17: 4 arcmin off-axis effective areas for the MS291+295, as measured with the PSpC in monochromatic setup.

	X-ray tests at PANTER on Nickel-Cobalt EM#3 (phase A) SIMBOL-X optic prototype						
Code:01/2009	INAF/OAB Technical Report	Issue:	2	Class	CONFIDENTIAL	Page:	27

5.3. HEW and W90

The HEW values of the two MS together exhibit qualitatively the same behaviour of the MS286 below 10 keV (Tab. 9), even if the resulting HEW values are the combination of two focal spots with different focal lengths. Also measurements at 2, 4, 5, arcmin off-axis were taken from the exposures *at the best-focus of the MS291+295 on-axis*. The W90 values at the same energy, as measured with the PSPC, are reported in Tab. 10. Like for the MS286 (Sect. 4.3), the HEW and W90 increases slowly with the photon energy as a consequence of the increasing relevance of the XRS. Moving the source off-axis, indeed, the HEW are larger than those on-axis only for $\omega = 2$ arcmin, then they decrease, though the increase of HEW is difficult to detect due to the statistical error. For the W90 the slow decrease starts at a 5 arcmin off-axis.

Tab. 9: on-axis and off-axis HEW (± 0.3 arcsec) of the MS291+295 at low energies (ROI < 180 arcsec).

HEW (arcsec)	Cu-L α (0.93 keV)	Al-K α (1.49 keV)	Ag-L α (2.98 keV)	Ti-K α (4.51 keV)	Cr-K α (5.41 keV)	Fe-K α (6.40 keV)	Cu-K α (8.05 keV)
on-axis	21.4	21.9	23.9	25.1	25.7	26.5	26.1
2 arcmin off-axis	21.6	21.6	23.6	25.8	26.0	26.7	26.9
4 arcmin off-axis	21.2	21.6	24.0	25.7	25.9	26.4	26.8
5 arcmin off-axis	20.8	20.8	22.9	25.0	25.0	25.2	25.7

We report the on-axis HEW measured with PSPC and TRoPIC (within a 170 arcsec radius ROI, see Sect. 4.3) at high energy in Fig. 18 and compare it with the HEW trends of the MS286 and of the whole EM#3 in Fig. 27. Notice that the increasing trend of the HEW at high energy is **very similar** to that of the EM#2 [AD4], made of two shells from the same mandrels, with the same HEW “bump” around 25 keV, and a quasi-stabilization at 40 arcsec between 35 and 40 keV. One should subtract, of course, the initial HEW at low energies, that was worse for the EM#2 because of the huge defocusing of the two shells ($\Delta f = 8$ cm). Nevertheless, in hard X-rays it is the X-ray scattering that dominates the HEW and the defocusing becomes less important.

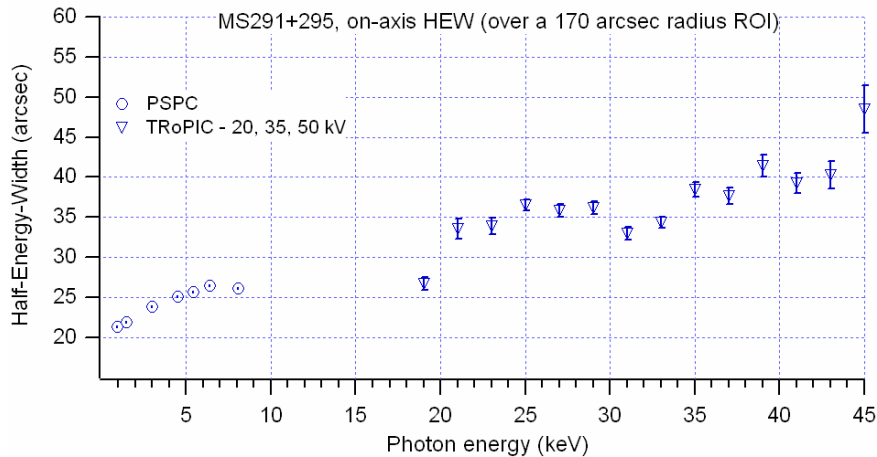




Fig. 18: on-axis HEW values for the MS291+295, as measured with the PSPC in monochromatic setup (circles) and in energy-dispersive setup with TRoPIC (triangles).

	X-ray tests at PANTER on Nickel-Cobalt EM#3 (phase A) SIMBOL-X optic prototype						
Code:01/2009	INAF/OAB Technical Report	Issue:	2	Class	CONFIDENTIAL	Page:	28

Tab. 10: on-axis and off-axis $W90$ (± 5 arcsec) of the MS291+295 at low energies ($ROI < 180$ arcsec).

W90 (arcsec)	Cu-L α (0.93 keV)	Al-K α (1.49 keV)	Ag-L α (2.98 keV)	Ti-K α (4.51 keV)	Cr-K α (5.41 keV)	Fe-K α (6.40 keV)	Cu-K α (8.05 keV)
on-axis	112	117	123	132	134	129	128
2 arcmin off-axis	116	127	125	135	139	132	132
4 arcmin off-axis	126	130	157	142	143	140	143
5 arcmin off-axis	126	129	139	139	140	138	137

	X-ray tests at PANTER on Nickel-Cobalt EM#3 (phase A) SIMBOL-X optic prototype						
Code:01/2009	INAF/OAB Technical Report	Issue:	2	Class	CONFIDENTIAL	Page:	29

6. Complete EM#3 optic (286+291+295)

6.1. The PSPC and TRoPIC views

The EM#3 (i.e. the three MSs together) has been tested in monochromatic (with the PSPC) and energy-dispersive setup (with TRoPIC) in-focus and intra-focus, on-axis and off-axis also at high energies. The images obtained in monochromatic setup (Fig. 19 and Fig. 20) and those recorded in energy-dispersive setup (Fig. 21 and Fig. 22) are very similar to those of the MS286 (Sect. 4.1) and the MS291+295 (Sect. 5.1). The in-focus images, in particular, exhibit a single focal spot, meaning that the three shells are well confocal, in spite of their different focal lengths. The HEW at 0.93 keV is **20.4 arcsec**, intermediate between that of the MS286 and the MS291+295 (more HEW measurements are reported in Sect. 6.3). The OOF images exhibit a ring deformation in the upper part, visible also in those of the MS291+295 (Fig. 12).

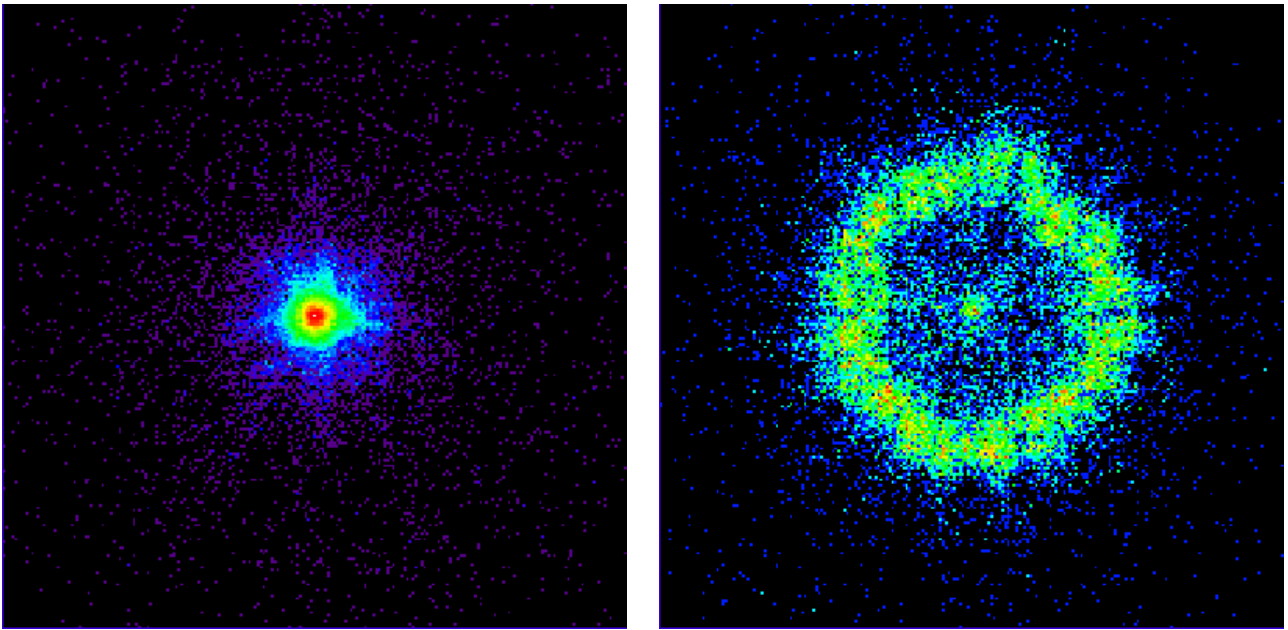



Fig. 19: the on-axis focal spot of the EM#3 at 0.93 keV (the Cu-La line), as seen by the PSPC. Logarithmic colour scale. (left) in focus, (right), 32.9 cm intra-focal.

The X-ray source settings and integration times have been the same used for of the MS286 (Sect. 4.1) and the MS291+295 (Sect. 5.1). The count rate accuracy for measurements in monochromatic mode is still 0.5%, with a few minutes integration time. Only for the out-of focus measurement on-axis the 20 kV setup was replaced with a 27 kV one with a 2 mA current and a 300 μm thick Ti filter, because the 20 kV exposure was likely to suffer from pileup problems due to the larger EA of the 3 shells together, with respect to the previous cases. In the 27 kV OOF setup, the pileup can be estimated to be less than 0.5% over all TRoPIC field. For the 20 kV infocus exposures (2 mA anode current, 500 μm Ti filter), the experimental pileup occurrence is instead less than 0.3 % over all the image (1% in the 9 central pixels).

All measurements in-focus and out-of focus were repeated at 35 kV and 50 kV, on-axis and with a 4 arcmin off-axis. In this way, we could probe the multilayer response (in terms of EA and HEW) also when the X-ray source was off-axis, and compare it with the theoretical modelization.

	X-ray tests at PANTER on Nickel-Cobalt EM#3 (phase A) SIMBOL-X optic prototype						
Code:01/2009	INAF/OAB Technical Report	Issue:	2	Class	CONFIDENTIAL	Page:	30

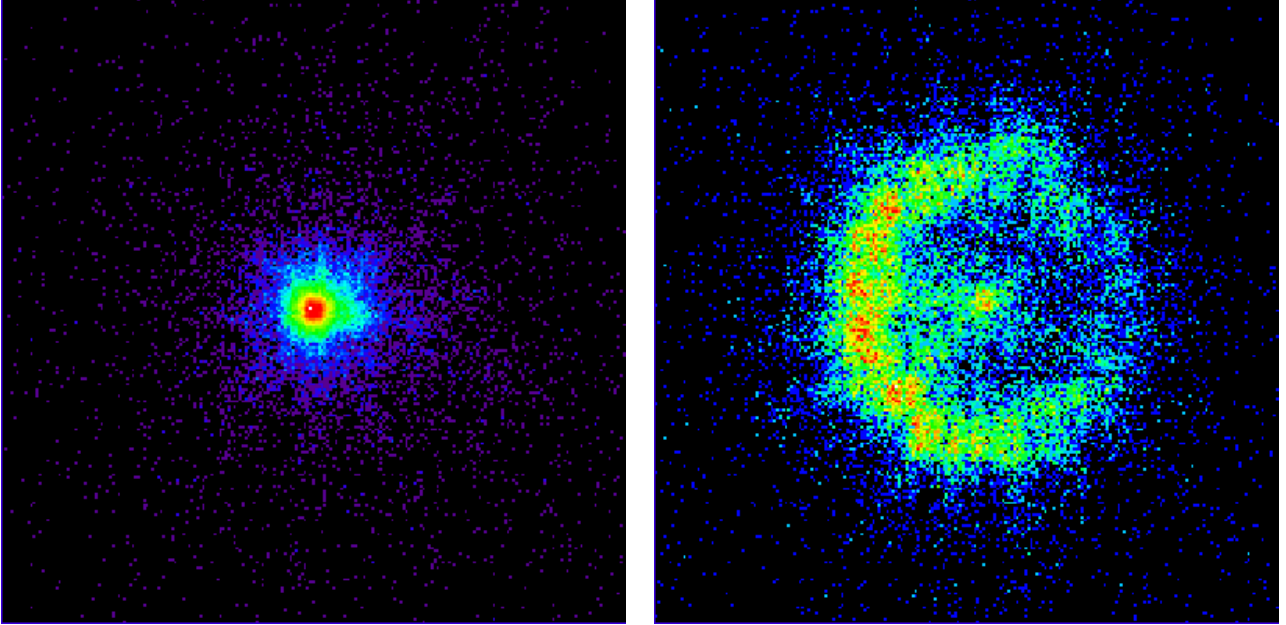


Fig. 20: 4 arcmin off-axis focal spot of the EM#3, as seen by the PSPC. Logarithmic colour scale. Same direction of rotation as Fig. 6. (left) in focus at 0.93 keV (the Cu-La line), (right), 32.9 cm intra-focal at 8.045 keV (the Cu-K α line).

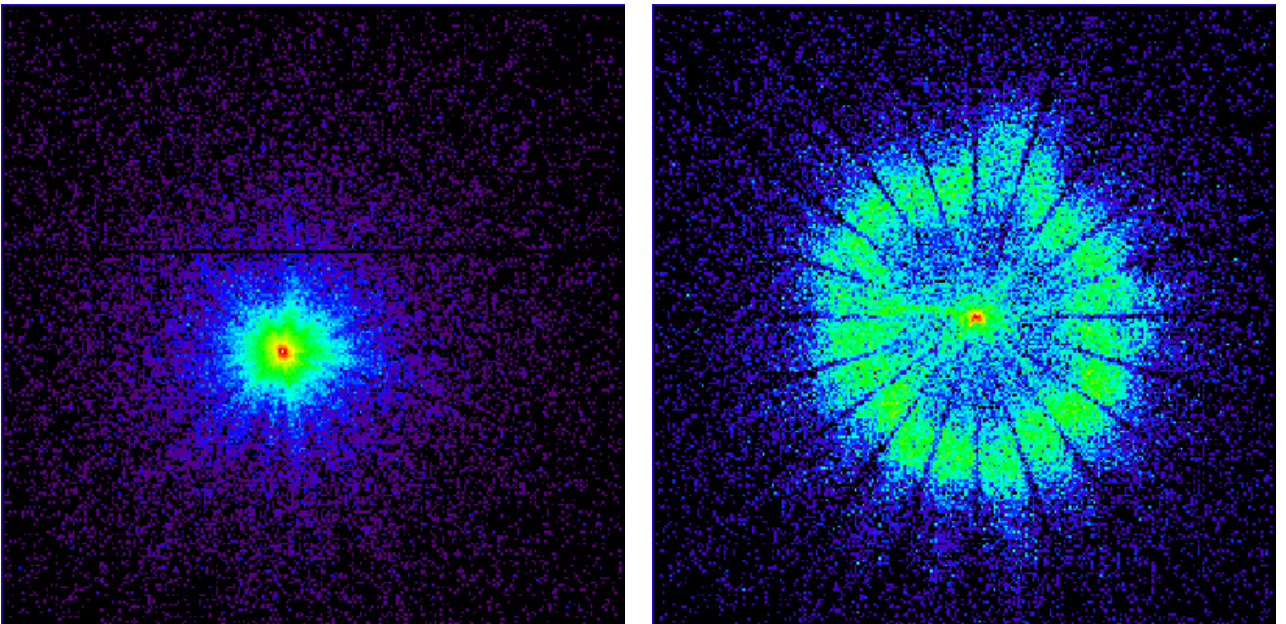



Fig. 21: on-axis focal spot of the EM#3 at seen by TRoPIC, with the X-ray source in 50 kV setup. Logarithmic colour scale. (left) in focus, (right), 32.9 cm intra-focal.

Also for the whole EM#3 the off-axis images exhibit the same features of the MS286 and the MS291+295, reported in Fig. 6 and Fig. 13. The in-focus images at 4 arcmin off-axis (Fig. 20 and Fig. 22) are essentially symmetric also concerning the distribution of scattered X-rays. The off-axis, intra-focal images show a relevant enhancement of reflectivity in sectors located at the left, due to the change of incidence angles over the mirror shells.

	X-ray tests at PANTER on Nickel-Cobalt EM#3 (phase A) SIMBOL-X optic prototype						
Code:01/2009	INAF/OAB Technical Report	Issue:	2	Class	CONFIDENTIAL	Page:	31

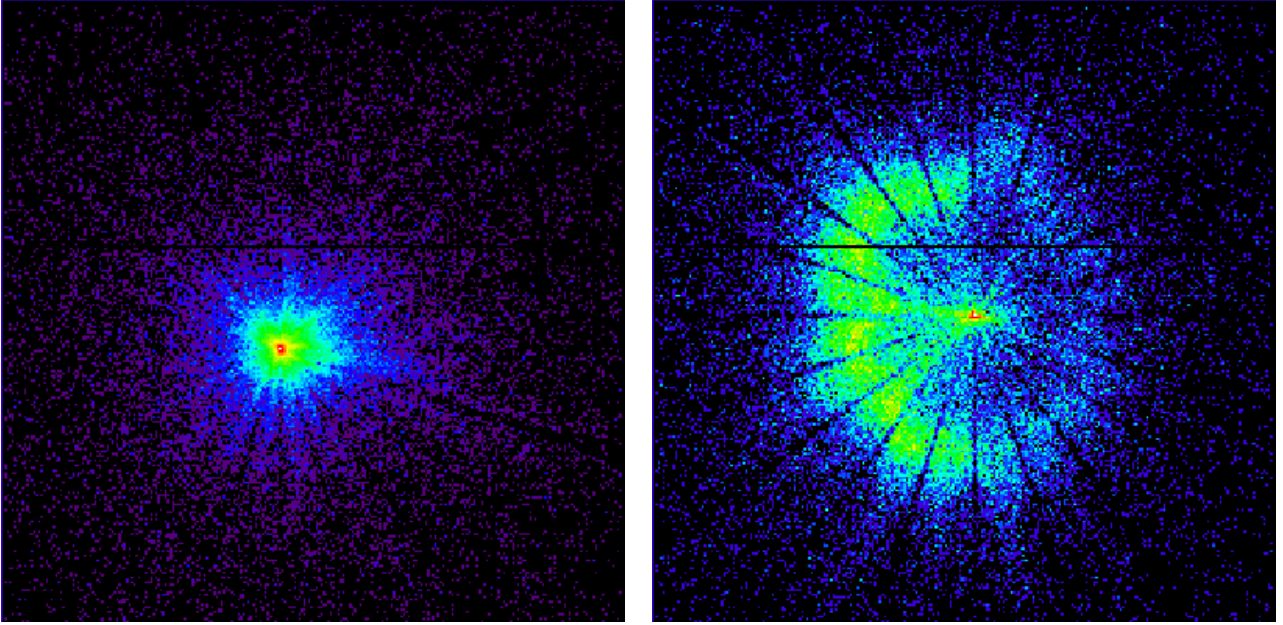


Fig. 22: 4 arcmin off-axis focal spot of the EM#3 at seen by TRoPIC, with the X-ray source at 50 kV setup. The direction of rotation is the same of Fig. 6. Logarithmic colour scale. (left) in focus, (right), 32.9 cm intra-focal.

6.2. Effective Areas

6.2.1. On-axis EA

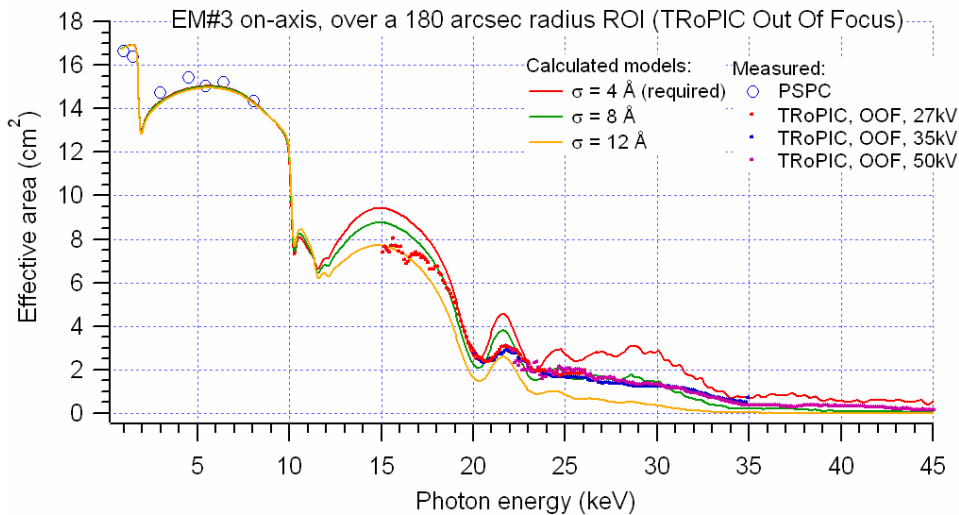



Fig. 23: the EA of the EM#3 on-axis, as measured in monochromatic setup with the PSPC and in energy-dispersive setup with TRoPIC, from OOF exposures.

Fig. 23 reports the on-axis effective area measured with the PSPC in monochromatic setup and with TRoPIC in energy-dispersive setup, with the X-ray source at 27, 35, 50 kV voltage bias, obtained from intra-focal measurements. The experimental data are in mutual agreement within the statistical error (a few % for the PSPC, 3% at 18 keV, 2% at 30 keV, 6% at 40 keV).

	X-ray tests at PANTER on Nickel-Cobalt EM#3 (phase A) SIMBOL-X optic prototype						
Code:01/2009	INAF/OAB Technical Report	Issue:	2	Class	CONFIDENTIAL	Page:	32

Like for the MS286 and MS291+295, the monochromatic measurements are in good agreement with the theory as they lie on the predictions within the statistical error, and did not provide a particular guess concerning surface roughness. The high-energy measurements also lie on the predicted curves, in particular they seem to fit quite well the theoretical curve with $\sigma \approx 8 \text{ \AA}$ from 17 keV on, while below this value they are more consistent with a higher roughness.

In general, for the 50 kV setup, we are missing 50% of the theoretically-required EA. In Fig. 24 we display a mosaic of 3 TRoPIC fields, showing, in addition to the intra-focal focal spot of the EM#3 (Fig. 21, right), also the neighbouring regions, mapped moving TRoPIC by 19.2 mm laterally. This has been done to evaluate the amount of scattering outside the central field: in fact, there is a non-negligible amount of scattered rays by the mirrors (they are not seen if the shutters are kept closed), as they represent together 5% of the count rate of the OOF image in the upper-left quadrant. This means *that we are losing 20% of the effective area at 23 to 50 keV already in the close vicinities of the central field*, i.e., within the nearby 360 arcsec. Hence, a 50% effective overall area loss due to XRS appears not so unlikely.

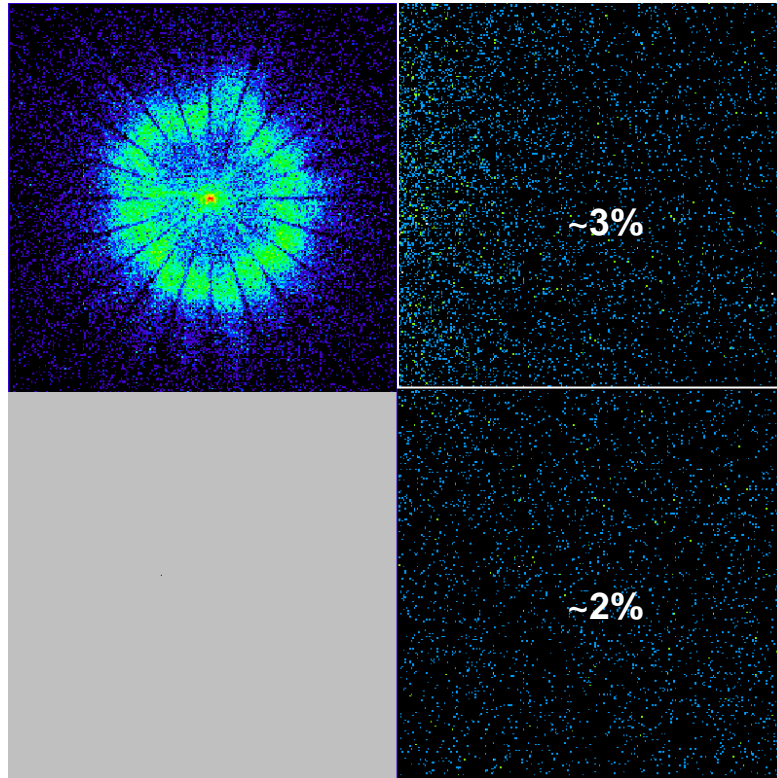



Fig. 24: a small mosaic of TRoPIC images around the intra-focal spot of the EM#3 in the 50 kV setup. The two lateral fields were taken with $\sim 1/2$ integration time and a source intensity 3 times as large as that of the focal image.

In-focus measurements (Fig. 25), in spite of the worse accuracy (4.5% at 30 keV), are more compliant with a 8 \AA roughness (the green, solid line) over all the energy range of measurement. Such a roughness value is still higher than the tolerable one ($\sigma \approx 4 \text{ \AA}$) represented by the red, solid line. Note that the effective area loss is still around 50% at 30 keV. The in-focus measurements with the source at 35 and 50 kV are almost unchanged with respect to the OOF case (Fig. 23).

	X-ray tests at PANTER on Nickel-Cobalt EM#3 (phase A) SIMBOL-X optic prototype					
Code:01/2009	INAF/OAB Technical Report	Issue:	2	Class	CONFIDENTIAL	Page: 33

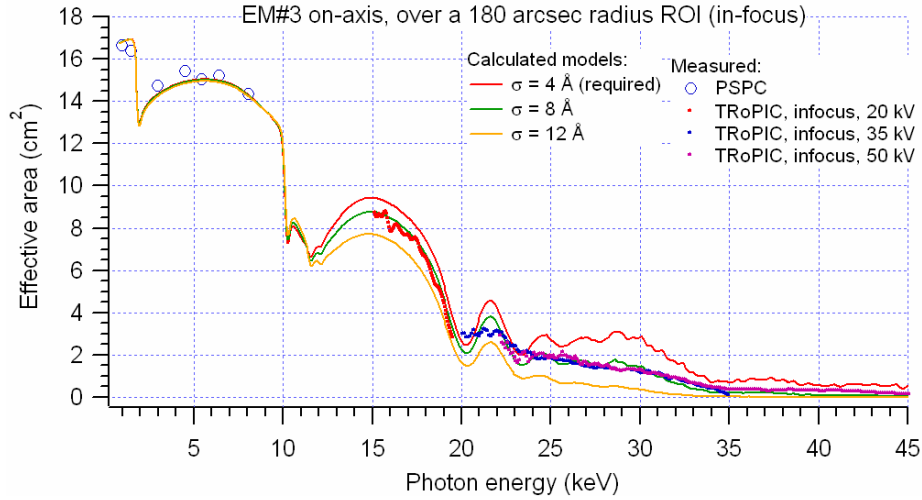


Fig. 25: the EA of the EM#3 on-axis, as measured in monochromatic setup with the PSpC and in energy-dispersive setup with TRoPIC, in-focus.

6.2.2. Off-axis EA

The EA results of the 4 arcmin off-axis measurement of the EM#3 in monochromatic (PSpC) and energy-dispersive (TRoPIC in focus) setup are plotted in Fig. 26. For the PSpC measurements, it can be seen that, like for the MS286 (Sect. 4.2.2) and MS291+295 (Sect. 5.2.2) separately, they lie on the theoretical predictions to a very good approximation. Below 10 keV, their values are almost unchanged with respect to the corresponding on-axis EA values, and they appear to be almost unaffected by the roughness of the mirrors. Also in this case we will not plot the EA below 10 keV for a 2 or 5 arcmin off-axis because they are almost unchanged with respect to those at 4 arcmin.

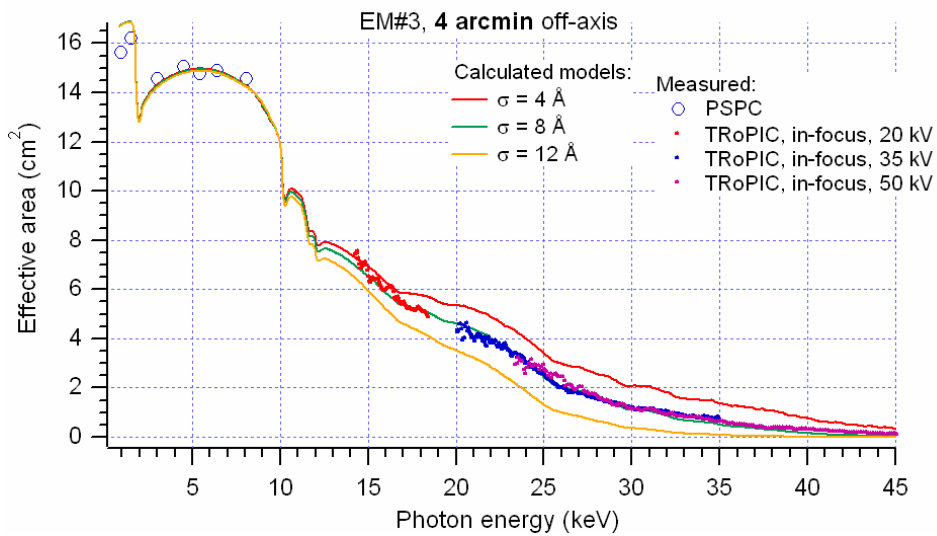



Fig. 26: the EA of the EM#3 4 arcmin off-axis, in-focus, as measured in monochromatic setup with the PSpC and in energy-dispersive setup with TRoPIC, in-focus. The different measurements are in mutual agreement within the statistical error and comply the theoretical model with a 8 Å surface roughness.

	X-ray tests at PANTER on Nickel-Cobalt EM#3 (phase A) SIMBOL-X optic prototype						
Code:01/2009	INAF/OAB Technical Report	Issue:	2	Class	CONFIDENTIAL	Page:	34

Beyond 10 keV, the situation changes, as it appears from TRoPIC data. The EA is completely different from the on-axis one (Fig. 25), with smoothed reflectance features because of the variation of the incidence angles over the mirror surfaces (Sect. 2.3). E.g., at 15÷17 keV the EA is higher on-axis, but at 20÷25 keV it is higher when the source is 4 arcmin off-axis. Nevertheless, it is *fully compliant with the theoretical model* assuming a $\sigma = 8 \text{ \AA}$, like the on-axis case (Sect. 6.2.1). This is another confirmation of the correctness of the multilayer structure assumption (Sect. 2.2).

6.3. HEW and W90

We report in Tab. 11 the low-energy measurements of the HEW for the EM#3, on-axis and off-axis, in monochromatic setup. Similar comments as for the MS286 (Sect. 4.3) and MS291+295 (Sect. 5.3) apply. Due to the small difference between the best foci of the MS286 or MS291+295 and that of the EM#3 ($\pm 1 \text{ cm}$), the HEW at 0.93 keV, on-axis, is intermediate between the two: 20.4 arcsec. It is closer, indeed, to that of the MS291+295 because they have an EA more than twice as large as that of the MS286 (see also Fig. 27 and Fig. 28). The HEW slowly increases with photon energy and off-axis up to 4 arcmin, then it starts to decrease.


The W90 values of the EM#3, measured in monochromatic setup, are listed in Tab. 12. The values are intermediate between those of the MS286 (Tab. 8) and those of the MS291+295 (Tab. 10) *Tab. 10: on-axis and off-axis W90 ($\pm 5 \text{ arcsec}$) of the MS291+295 at low energies (ROI < 180 arcsec).* Also in this case we see an increase of the W90 with the photon energy and with the off-axis up to 4 arcmin, followed by a decrease at 5 arcmin.

Tab. 11: on-axis and off-axis HEW ($\pm 0.3 \text{ arcsec}$) of the EM#3 at low energies (ROI < 180 arcsec).

HEW (arcsec)	Cu-L α (0.93 keV)	Al-K α (1.49 keV)	Ag-L α (2.98 keV)	Ti-K α (4.51 keV)	Cr-K α (5.41 keV)	Fe-K α (6.40 keV)	Cu-K α (8.05 keV)
on-axis	20.4	21.0	22.7	24.4	25.0	25.1	25.6
2 arcmin off-axis	20.4	21.3	23.1	24.6	25.2	25.0	25.7
4 arcmin off-axis	21.3	21.6	23.1	24.7	25.3	26.5	26.4
5 arcmin off-axis	20.0	20.9	22.9	25.4	24.8	25.1	25.4

Tab. 12: on-axis and off-axis W90 ($\pm 4 \text{ arcsec}$) of the EM#3 at low energies (ROI < 180 arcsec).

W90 (arcsec)	Cu-L α (0.93 keV)	Al-K α (1.49 keV)	Ag-L α (2.98 keV)	Ti-K α (4.51 keV)	Cr-K α (5.41 keV)	Fe-K α (6.40 keV)	Cu-K α (8.05 keV)
on-axis	102	111	113	121	127	125	128
2 arcmin off-axis	108	113	121	130	130	127	128
4 arcmin off-axis	116	128	127	135	136	137	131
5 arcmin off-axis	108	125	128	132	134	131	130

	X-ray tests at PANTER on Nickel-Cobalt EM#3 (phase A) SIMBOL-X optic prototype						
Code:01/2009	INAF/OAB Technical Report	Issue:	2	Class	CONFIDENTIAL	Page:	35

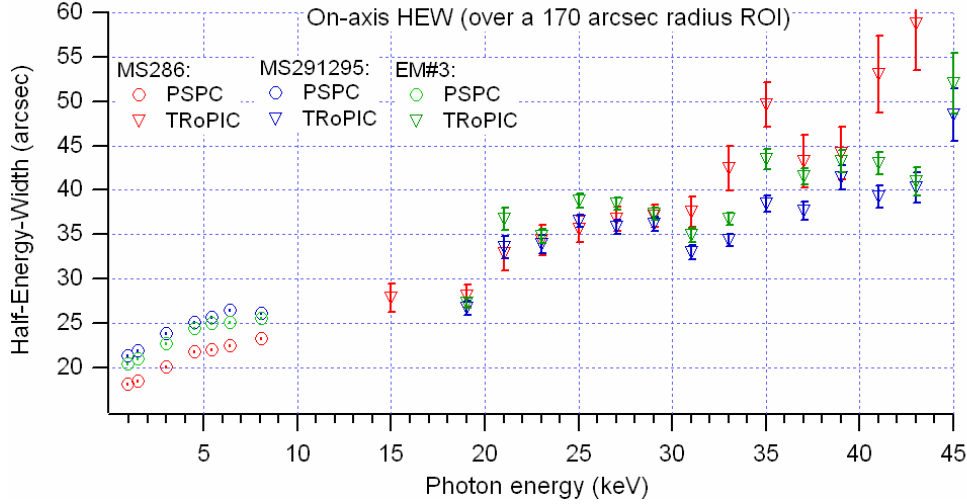



Fig. 27: comparison of the on-axis HEW for the MS286, MS291+295, EM#3, as measured with the PSPC in monochromatic setup, and with TRoPIC in energy-dispersive setup.

We report in Fig. 27 the on-axis HEW of the EM#3, as measured with PSPC at low energies and TRoPIC at high energy. We also over-plot the HEW trend of the MS286 (Sect. 4.3) and those of the MS291+295 (Sect. 5.3), at the respective best foci (Sect. 3), in monochromatic (circles) and energy-dispersive (triangles) setup.

The EM#3 has an intermediate behaviour between the MS286 and the pair MS291+295 (the latter is also very similar to the EM#2 in terms of HEW [AD4]), but it is always more similar to the latter as the two mirrors have together a larger EA, so they weight more in the overall HEW. All HEW trends seemingly tend to “saturate” up to 20 keV, then start to increase again. Oscillations in the HEW are probably related to a modulation of the X-ray scattering, by interference of scattered X-rays by the interfaces in the multilayer. Note that the MS286 is the best shell at low energies (even if the performances of the other two are biased by a mutual defocusing) but it becomes the worst one at high energies, probably due to a higher roughness.

In Fig. 28 we summarize the HEW trend for the whole EM#3 with the source 4 arcmin off-axis, taken from the exposures at the best-focus of the EM#3 on-axis, in monochromatic setup with the PSPC (e.g. Fig. 20) and in polychromatic setup with TRoPIC (e.g. Fig. 22). We also overplotted the HEW trend of the MS296 and that of the pair MS291+295 in monochromatic setup for a 4 arcmin off-axis. High energy data off-axis are available only for the EM#3. It is remarkable, comparing Fig. 27 and Fig. 28, that at high energies the HEW trend of the EM#3 off-axis resembles the on-axis one, with values falling in the same range, but with *smoothed oscillations*. The same smoothing was observed in the EA off-axis (Sect. 6.2.2). This is expected if the undulations in the HEW trend are caused by interference of scattered X-rays in the multilayer: the off-axis causes a spread of the incidence angles on the MSs and shifts the position of maxima and minima in the XRS diagrams of different sectors of the mirrors. Then the interference features would be averaged out more and more as the X-ray source moves off-axis; this is exactly what is being observed in the present case.

	X-ray tests at PANTER on Nickel-Cobalt EM#3 (phase A) SIMBOL-X optic prototype					
Code:01/2009	INAF/OAB Technical Report	Issue: 2	Class CONFIDENTIAL	Page: 36		

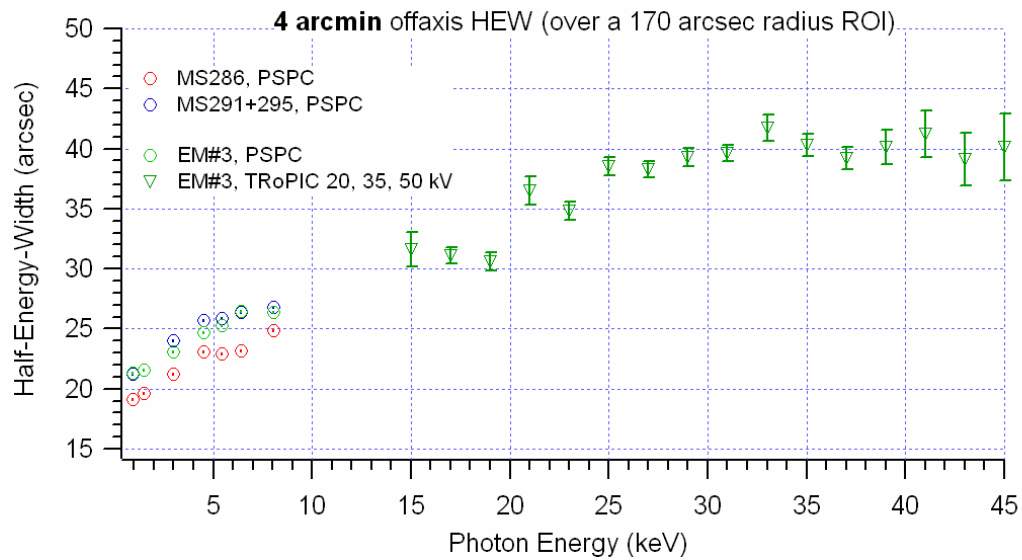



Fig. 28: 4 arcmin off-axis *HEW* values for the *MS286*, *MS291+295*, *EM#3*, as measured with the *PSPC* in monochromatic setup (circles) and for the *EM#3* in energy-dispersive setup with *TROPIC* (triangles).

	X-ray tests at PANTER on Nickel-Cobalt EM#3 (phase A) SIMBOL-X optic prototype						
Code:01/2009	INAF/OAB Technical Report	Issue:	2	Class	CONFIDENTIAL	Page:	37

7. Final remarks

The results reported in the present report highlighted positive aspects, like the agreement between the predicted and measured EA values at low energies, on-axis and off-axis, but also some points on which future developments of the project should be focused:

- ✓ A detailed study of the variation of focal lengths of mirror shells from the electroforming stage to the multilayer coating. In particular the attention should be drawn on the stress introduced by the multilayer coating.
- ✓ Investigation of the surface roughness evolution at each step of the mirror shell production, in order to identify with certainty the XRS as the cause of the HEW degradation and the EA loss at high energies. The study should also be able to explain the different performances, in terms of EA, of the in-focus and out-of focus measurements in hard X-rays. Moreover, it should also identify the production stage responsible for roughness degradation and to suggest how to correct it, in order to fulfill the imaging quality requirements for SIMBOL-X.